STRUCTURAL STYLE VARIATIONS IN THE HIMALAYAN FRONT:

IMPLICATIONS FOR WEDGE-TOP DEPOSITION, NEPAL

A Thesis

Presented to

the Faculty of the Department of Earth and Atmospheric Sciences

University of Houston

In Partial Fulfillment

of the Requirements for the Degree

Master of Science

By

Laura P. Unverzagt

May 2012

STRUCTURAL STYLE VARIATIONS

IN THE HIMALAYAN FRONT:

IMPLICATIONS FOR WEDGE-TOP

DEPOSITION, NEPAL

_____

Laura P. Unverzagt

APPROVED:

_____

Dr. Michael Murphy, Chairman

_____

Dr. Alexander Robinson

_____

Dr. Shane Prochnow

Chevron Corporation, Midland, Texas

_____

Dean, College of Natural Sciences and Mathematics

ACKNOWLEDGEMENTS

My special thanks go to Dr. Michael Murphy for his guidance and inspiration during this study. I would like to thank Dr. Shane Prochnow for guidance using ArcGIS which allowed me to create detailed and accurate figures. Many thanks go to Ana Krueger for meeting with me multiple times to help me learn how to model using 2DMove. My thanks goes to Midland Valley for providing student licenses for Move and 2DMove so I could created detailed kinematic models and cross sections. My sincerest thanks go to Dr. Alex Robinson for his thorough review and constructive feedback of my research. My deepest gratitude goes to my loving husband who supported me through the entire process. I could not have completed this project without the unwavering support of faculty and family.

STRUCTURAL STYLE VARIATIONS IN THE HIMALAYAN FRONT:

IMPLICATIONS FOR WEDGE-TOP DEPOSITION, NEPAL

An Abstract of a Thesis

Presented to

the Faculty of the Department of Earth and Atmospheric Sciences

University of Houston

In Partial Fulfillment

of the Requirements for the Degree

Master of Science

By

Laura P. Unverzagt

May 2012

ABSTRACT

Deformation at the front of the Himalayan thrust wedge is focused along the Main Frontal Thrust (MFT) resulting in shortening of the Neogene foreland basin deposits since the Pleistocene. This research investigates variations in structural style along the MFT in the Dang Valley region, west-central Nepal, and how these variations affect the distribution of modern wedge-top sediment depocenters.

Four kinematic models and cross sections were constructed to evaluate plausible geometric and kinematic histories. Three structurally distinct regions are recognized: 1) the western section distinguished by north-dipping imbricate thrusts; 2) the central section characterized by south-dipping back thrusts that structurally confine the southern margin of the Dang Valley; and 3) the eastern section distinguished by north-dipping imbricate thrusts and south-dipping back thrusts that form along a shallow detachment resulting in a composite pop-up structure.

Neogene shortening estimates across the study area range from 47% to 40%. Derived shortening rates that range from 20 mm/yr to 14 mm/yr are consistent with modern geodetically derived India-Eurasia convergence rate across the Himalaya. This implies that in this region most of the shortening since initiation of tectonic activity ca. 2.3 Ma, has been accommodated between the Main Boundary thrust (MBT) and the MFT along a single basal detachment known as the Main Himalayan Thrust (MHT).

Two transfer zones are the most plausible features to explain the along-strike variation in structural style within the study area. From west to east these are: 1) the West Dang Transfer Zone (WDTZ), interpreted to be a complex zone of strike-slip faults and lateral ramps which may transfer strain to a deeper detachment level to the east; and 2)

the Masot Khola Transfer Zone (MKTZ), interpreted to transfer strain along a lateral ramp to a deeper basal detachment and a secondary shallow detachment surface to the east.

The results of this study suggest there is a relationship between changes in structural style and wedge-top development. Abrupt changes in distribution of wedge-top sediments are coincident with changes in structural style.

CONTENTS

LIST OF ABBREVIATIONS

DEM: Digital Elevation Model

FPF: Fault Propagation Fold

ID: Internal Decollement

Ls: Lower Siwalik

MBT: Main Boundary Thrust

MCT: Main Central Thrust

MDT1: Main Dun Thrust 1

MFT: Main Frontal Thrust

MHT: Main Himalayan Thrust

MKTZ: Masot Khola Transfer Zone

Ms: Middle Siwalik

RT: Ramgarh Thrust

SKT: Silling Khola Thrust

ST: Sit Khola Thrust

STDS: South Tibetan Detachment System

Us: Upper Siwalik

USGS: United States Geological Survey

WDTZ: West Dang Transfer Zone

1. INTRODUCTION

Our study shows there are striking differences in the structural style along the MFT, the zone of most compressional activity along the Himalayan orogen. The Himalaya are the result of active collision between the Indian and Asian plates. The Main Frontal Thrust (MFT) extends greater than 2000 km from Bhutan to the northwest Himalaya and strikes parallel to the thrust front. Important aspects of the trace of the MFT are the numerous salients and reentrants.

The study area (Figure 1) is located north of the MFT and south of the Main Boundary Thrust (MBT) in the Subhimalayan Zone. The MFT involves rocks of the Siwalik Group which are divided into the upper (Us), middle (Ms), and lower (Ls) Formations (Figure 2). The Ls and middle Ms Formations are interpreted as foredeep deposits consisting of increasingly proximal transverse river deposits. The upper Siwalik (Us) Formation is composed of megafan conglomerates and represents the transition from foredeep to synorogenic wedge-top deposits (DeCelles et al., 1999a). Quaternary alluvium deposits are found above the upper Siwalik in present day topographic lows.

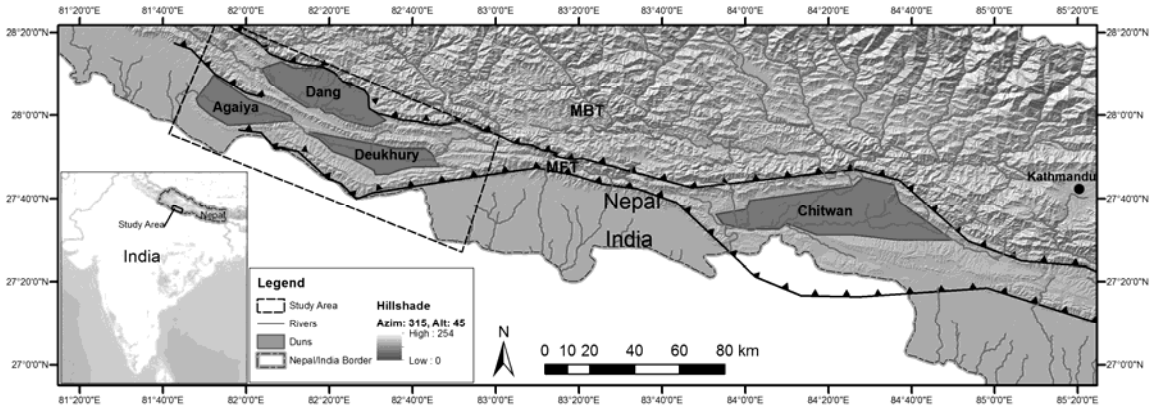

Figure 1: Subhimalayan Zone Duns. The trace of the MFT is characterized by salients and reentrants. The duns form as piggy-back basins north of the salient and are characterized by axial rivers and Quaternary sediments.

Active deposition of Quaternary sediments occurs by alluvial fan systems and accumulate in local depocenters within intermountain basins referred to as duns. Several duns are recognized across the Himalaya and generally occur several 10's of kilometers north of the southern topographic expression of the MFT. Examples of duns are the Dang Valley, the Deukhury Valley, Agaiya Valley, and Chitwan Valley (Figure 1).

This research investigates the geometry and kinematic evolution of the study area by compiling previously published geologic maps and constructing kinematic models to address the following questions:

1. What are the structural styles that accommodate shortening?
2. Are there any along strike variations in structural style?
3. Is there a relationship between wedge-top deposition and structural style?

In this study we present research on variations in structural styles that accommodate shortening in the Subhimalyan zone and how variations affect wedge-top placement. A better understanding of the structural styles will constrain estimates of the amount of shortening accommodated north of the MFT and south of the MBT from the Pleistocene to present day.

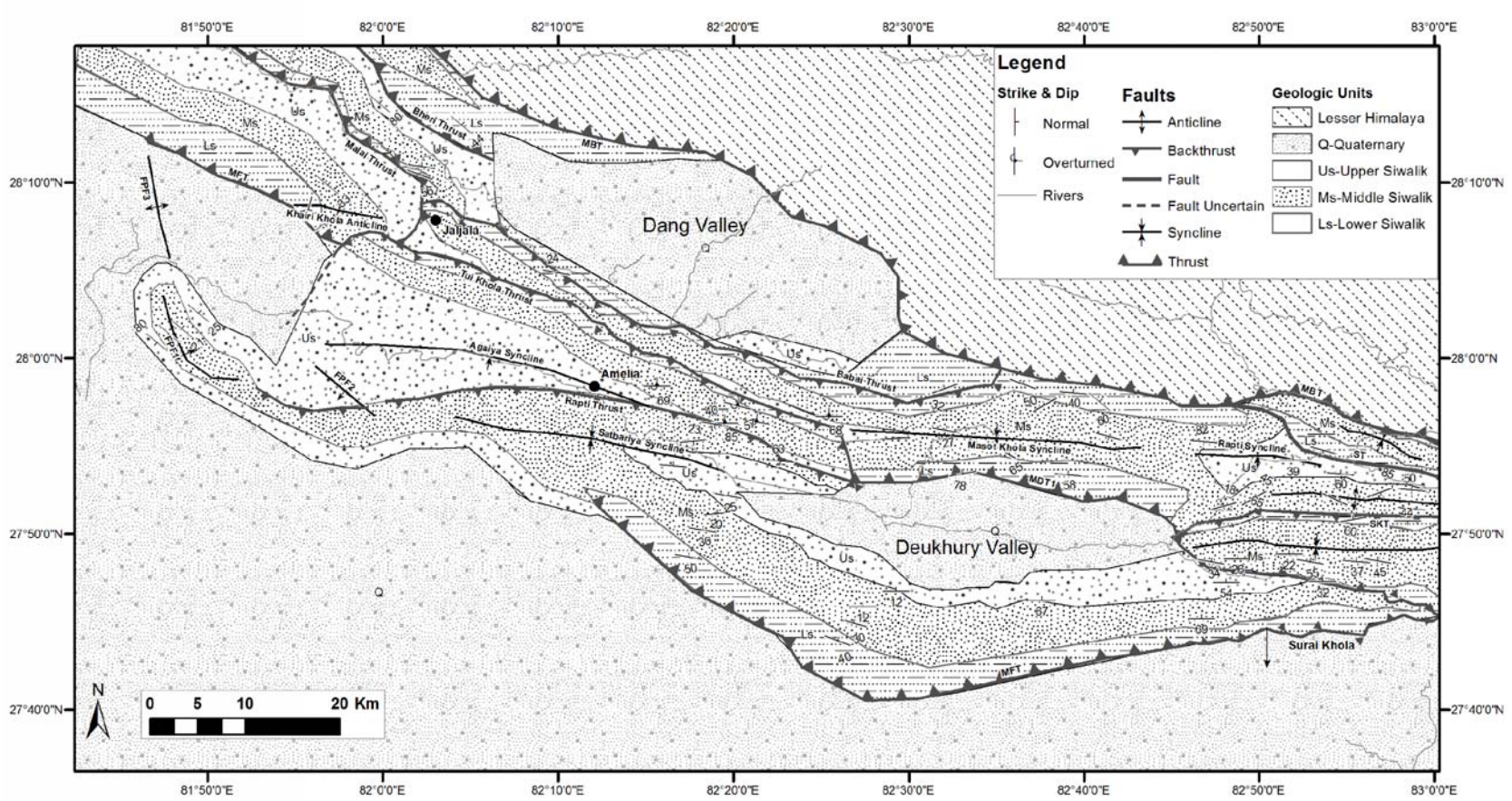

Figure 2: Geologic Map of the Study Area. The Siwalik thrust belt located in mid-western Nepal. Interpretations are compiled from multiple published geologic maps (Geologic Map of Nepal (scale: 1:1,000,000); Nakayama and Ulak, 1999; Mugnier et al., 1999; Regumi et al., 2011). See list of Abbreviations.

2. TECTONIC FRAMEWORK

2.1. Tectonostratigraphic Units

The Himalayas can be divided into five major tectonostraigraphic zones (Figure 4); the Terai Zone, the Siwalik Group (Subhimalaya), Lesser Himalayan zone (Upper and Lower), the Greater Himalayan Zone, and the Tibetan-Tethys Zone (Upreti, 1999: Robinson et al., 2006). These zones are distinguished based on lithology and structural history (Upreti, 1999).

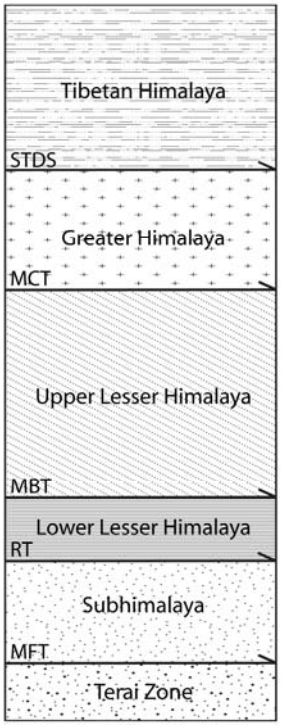

Figure 3: Himalayan tectonostratigraphic zones. The faults between zones are shown with arrows.

The Terai Zone is bounded to the north by the MFT and is the most recent alluvium at the northern edge of foreland basin. This Formation has an average thickness of 1,500m. The sediments are Pleistocene to recent alluvium. The Himalayan thrust front is currently propagating into the Terai zone with blind thrusts forming beneath the sediments (Upreti, 1999).

The Siwalik Group also known as the Subhimalaya Zone contains one of the largest foreland basin deposits on earth. This zone is comprised of Neogene to Quaternary fluvial sediments. The Siwalik zone is bounded to the north by the MBT and to the south by the MFT. These sediments have been broadly folded, faulted, and thrust over the Terai Zone along the MFT (Upreti, 1999).

The Lesser Himalayan zone lies between the MBT and the Main Central Thrust (MCT) and is composed of Precambrian sedimentary rocks and younger sedimentary successions that have been thrust over the Siwalik group rocks. A widespread unconformity marks the boundary between the Lower and Upper Lesser Himalayan deposits. The Ramgarh thrust (RT) places the Kushma and Ranimata Formations of the Lower Lesser Himalaya above the Upper Lesser Himalaya throughout Nepal. Deposition of the Dumri Formation foreland basin deposits in the early Miocene records the emergence of the Himalaya from the beneath the sea and marks the top of the Upper Lesser Himalayan Zone (Upreti, 1999; Robinson et al., 2006).

The Greater (Higher) Himalayan Zone lies between the MCT and the South Tibetan Detachment System (STDS). It is composed of Pre-Cambrian to Paleozoic gneisses, paraneisses, schists, marble, and Cenozoic Leucogranites. These units have been thrust along the MCT to the south and are observed in multiple klippen in southern Nepal (Upreti, 1999; Robinson et al., 2006).

The northernmost zone is the Tibetan Himalaya Zone. Rocks of the Tibetan Himalayan Zone were deposited as part of the Indian passive continental margin (Liu and Einsele, 1994; Upretti, 1999). This zone is comprised of low grade metamorphosed

sedimentary rocks. This Formation is bounded to the North by the Indus-Yarling Suture and to the south by the STDS. The STDS is a north-dipping normal fault system.

2.1.1. *Cross Section A-A'*

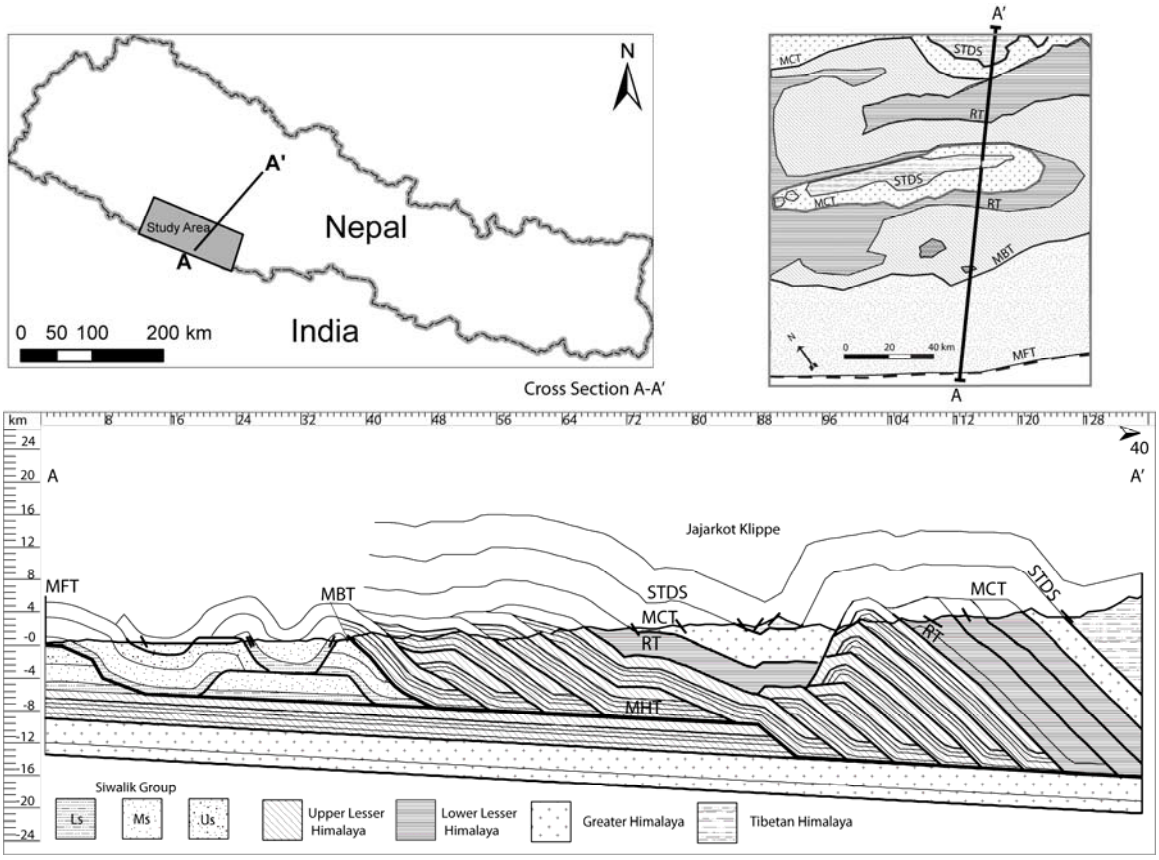

Figure 4: 2DMove Regional Cross Section. Cross section A-A' incorporates data north of the study area to the STDS. Siwalik Region is between the MFT and the MBT. Upper Lesser Himalayan duplexing creates the Jajarkot klippe in the north.

Cross Section A-A' illustrates the structural architecture of the Himalayas and the thrust wedge. The MHT consists of ramps and flats along which displacement creates duplexing, thickening the wedge to the north. In the south the MFT represents the southern extent of the thrust wedge.

The Tibetan Himalaya rocks in the STDS hanging wall lie structurally above the Greater Himalayan rocks in the MCT hanging wall. The RT hanging wall contains rocks of the Lower Lesser Himalaya which are structurally below the Greater Himalyan rocks above the MCT. The STDS, MCT, and RT hanging walls are interpreted to be roof thrusts uplifted by duplexing in the Upper Lesser Himalayan rocks (Figure 3) (Robinson, 2001; Robinson, 2008). Figure 3 illustrates significant duplexing to the north and south of the Jajarkot klippe uplifting and exposing roof thrust sheets to significant erosion. The roof thrust sheets (STDS, MCT, and RT) are only preserved in the Jajarkot klippe which is a topographic low formed as a result of less duplexing of the Upper Lesser Himalaya beneath the klippe than to the north and south.

The Main Boundary Thrust (MBT) is the southernmost extent of the Lesser Himalayan duplexing (Robinson, 2008). South the MBT is the Subhimalayan region which consists of synorogenic Siwalik deposits. Faulting in this region is interpreted in Figure 3 to consist of foreland propagating thrusts and wedge deformed pop-up structures.

2.2. Kinematic Evolution of Himalayan Thrust Wedge

2.2.1. *Critical Taper*

Structural evolution of the Subhimalayan Zone is governed by the dynamics of the Himalayan thrust wedge (Davis et al., 1983; Dahlen, 1990; Hodges et al., 2001; Larson et al., 2010). Compressional tectonics in the Himalayan region has resulted in thrusting and shortening which has built up an orogenic wedge creating an increase in gravitational potential energy (Hodges et al., 2001; Larson et al., 2010). Critical Taper wedges build up until they reach an angle that is steep enough to initiate sliding known as

the critical angle. Supercritical failure occurs when the wedge taper is above the critical angle as to decrease the angle of the wedge and reduce gravitational potential energy (Davis et al., 1983). One model suggests that evidence of supercritical failure is expressed by normal faulting along the STDS and foreland propagation in the Himalayas from the Middle Miocene to present day along the MHT/MFT (Larson et al., 2010).

2.2.2. *Himalayan Foreland Basin Development*

The development of the large Himalayan thrust wedge created a tectonic load that formed the peripheral foreland basin system. The Himalayan peripheral foreland basin system has four depozones with increasing distance from the thrust wedge; wedge-top, foredeep, forebulge, and back-bulge (Figure 5), that formed in response to the tectonic load of the thrust wedge (DeCelles and Giles, 1996; Horton and DeCelles, 1997; Currie, 1997). As the thrust wedge developed and propagated southward, the depozones migrated leaving a trace of this migration in the stratigraphic record interpreted as a large unconformity (DeCelles et al., 1999a).

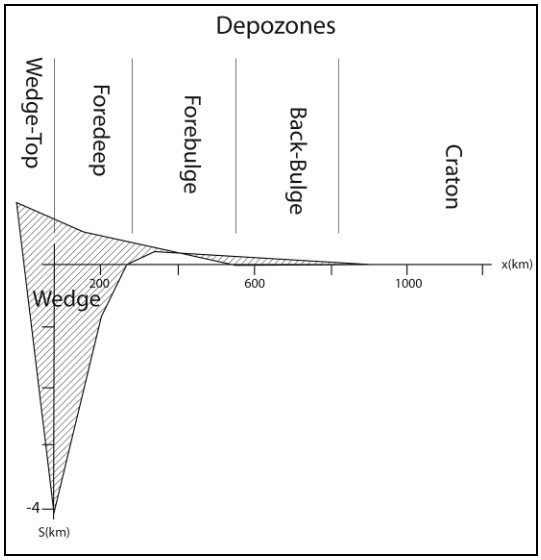

Figure 5: Modeled cross section of peripheral foreland basin illustrating depozones (DeCelles and Giles, 1996). Distance from orogenic wedge (x) versus regional subsidence (S). Model is based on equations by Turcotte and Schubert (1982). Figure modified from Decelles et al. (1998).

Based on sedimentological, provenance, and subsidence data, the timing of foreland basin development and crustal thickening is thought to be around middle Eocene time (DeCelles et al., 1999a). The stratigraphy in the peripheral foreland basin consists of upward coarsening deposits with initially low subsidence rates in a passive margin setting, to an increase in subsidence in the foredeep depozone. These units are known as the Amile, Bhainskati, Dumri Formations, and Siwalik group (DeCelles et al., 1999a).

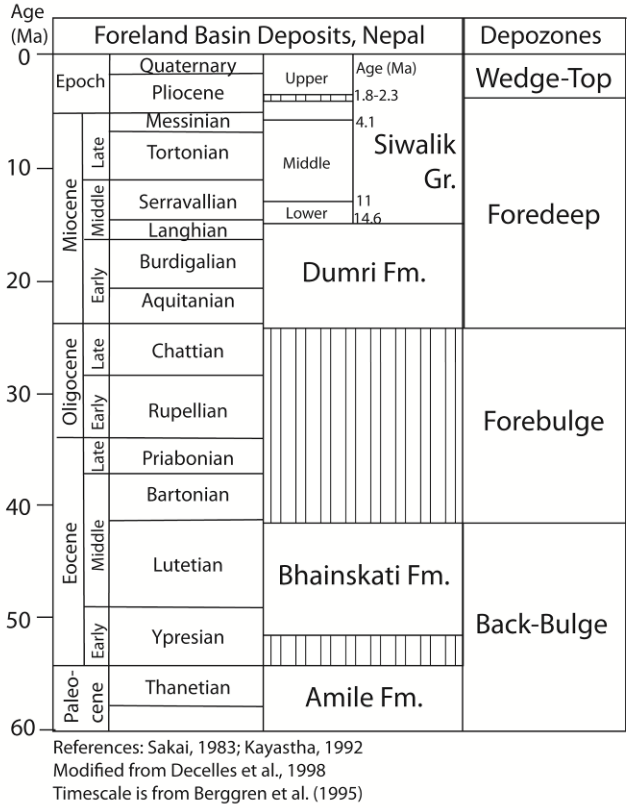

Figure 6: Stratigraphy of the Tertiary rocks in Nepal. Large unconformity illustrated with vertical lines created by the migration of the forebulge.

A large unconformity exists in the peripheral foreland basin and is marked by the absence of the Eocene-Oligocene section (Figure 6). The unconformity is proposed to be the result of a forebulge that formed after the collision event (Powell and Conaghan, 1973; Crampton and Allen, 1995; DeCelles et al. 1999a). The sediments deposited below the unconformity are interpreted to be from the back-bulge and make up the Bhainskati

Formation. Sediments deposited above the unconformity are interpreted to be part of the Dumri Formation and the lower and middle Siwalik Group which represents the distal to proximal foredeep. The wedge-top deposits are deformed conglomerate alluvial fans composed of the upper Siwalik Group (DeCelles et al., 1999a).

2.3. Siwalik Group

2.3.1. *Lithostratigraphy*

The Siwalik Group is located in southern Nepal south of the MBT and is divided into the following formations from oldest to youngest: Bankas Formation, Chor Khola Formation, Surai Khola Formation, Dobata Formation, and the Dhan Khola Formation (Dhital et al, 1995). These formations are often lumped into the lower (Bankas), middle (Chor Khola and Surai Khola), and upper (Dobata and Dhan Khola) Siwaliks (Auden, 1935). The Siwalik Group shows a coarsening upward sucession and an interpreted decrease in distance to the thrust front which is evidence of continuing southward propagation in the Himalayas (Regumi et al., 2011; Mugnier et al., 1999). The lower Siwalik Formation is the most distal member and consists of silty and sandy units that transition into the more proximal sandstones of the middle Siwalik formation. The conglomerates of the upper Siwaliks represent the proximal fluvial megafan environment (Mugnier et al., 1999).

The Bankas Formation of the lower Siwalik group consists of fine to very fine sandstones and red to purple mudstones which indicate subaerial exposure as paleosols. The environment of deposition is the distal portion of a channel system associated with a megafan (Delcaillau et al., 1987; Tandon, 1990). The exposed thickness of the Bankas Formation is controlled by thrusting. Many local thrusts and back thrusts eliminate some

sections and repeat others (Regumi et al., 2011). Thickness measurements vary from greater than 730 m south the Dun of Dang (Regumi et al., 2011) to greater than 585 m in the Surai Khola area (Dhital et al., 1995).

The Chor Khola Formation of the middle Siwalik group mainly consists of fine-to coarse-grained sandstones and red-purple-gray mottled mudstone. Deposits consist of meandering channel and floodplain deposits (Delcaillau et al., 1987; Tandon, 1990). The upper portion of the formation contains peat and organic material. The Chor Khola formation is marked by the first appearance of sandstone beds greater than 4 m thick and the sandstone units continue to thicken up section (Regumi et al., 2011). The thickness varies from 1500 m south of the Dun of Dang (Regumi et al., 2011) to 1200 m in the Surai Khola area (Dhital et al., 1995).

The Surai Khola Formation of the middle Siwalik group is composed of 80% sandstone and 20% mudstone with marls and shales. The sandstones of this formation are multistory coarse- to very coarse-grained units with a salt and pepper appearance due to biotite and quartz grains. The thickness of this formation in outcrop is 1,300 m south of the Dang Valley but varies greatly due to faulting. Cross laminations are abundant and indicate overturning in the back thrust sheets south of the Dang Valley (Regumi et al., 2011). The depositional environment is a meandering river system with high bed load which deposited thick multistory channel systems (Delcaillau et al., 1987; Tandon, 1990).

The Dobatta Formation of the upper Siwalik group consists of mostly yellow-brown, gray mudstone (63%) with some thin coarse-grained sandstone (23%) and conglomerate (14%) (Regumi et al., 2011). The thickness of the Dobata formation varies from 385 m (Regumi et al., 2011) south of the Dun of Dang to 750 m in the Surai

Khola area (Dhital et al., 1995). The environment of deposition is a meandering channel system (Mugnier et al., 1999).

The Dhan Khola formation of the upper Siwalik group consists mainly of coarse conglomerates and light brown sandstones. The thickness of the section and individual beds decreases from north to south. In the north boulder-size conglomerates are present with increasing mudstone and pebble conglomerates to the south (Regumi et al., 2011). The thickness is around 450 m just south of the Dang Valley (Regumi et al., 2011) and thickens to the west to 1100 m (Dhital et al.,1995) in the Surai Khola Region. The environment of deposition is proximal fans (Delcaillau et al., 1987; Tandon, 1990).

2.3.2. *Chronology*

The ages of the rocks that form the Siwalik Group (Figure 6) have been well established by detailed studies using magnetostratigraphy (Gautam and Appel, 1984), paleomagnetic studies (West and Munthe, 1981; Harrison, 1993) and biostratigraphy (Corvinus, 1998). Dhital et al. (1995) established the detailed stratigraphy of the Siwaliks and their corresponding chronology. The boundary between the Bankas and Chor Khola Formations (lower and middle Siwalik) is approximately 11 Ma. The boundary between the Chor Khola and the Surai Khola Formations is approximately 7 Ma. The boundary between the Surai Khola and Dobata Formations (middle and upper Siwalik) is approximately 4.1 Ma. Between the Dobata and Dhan Khola Formations of the Us is a 1.8 and 2.3 Ma unconformity. In the Deukhury Valley region ~~the~~ chevron~~s~~ folds in the Dobatta Formation (Appel et al., 1991) are clearly truncated by the flat lying conglomerates of the Dhan Khola Formation (Mugnier, 1999). Evidence of this truncation is not observed in the Surai Khola section (Appel et al., 1991) because the

unconformity paralleled the beds (Mugnier et al., 1999). Mugnier et al. (1999) has identified other locations in the study area where unconformities exist just below the conglomerates of the Upper Siwalik and has concluded that the presence of unconformities likely represent the initiation of tectonic activity in the Subhimalayan region.

2.3.3. *Thickness of the Siwalik Group in the Study Area*

The environment of deposition of the Siwalik group indicates that variations in thicknesses are likely the result of the formation of isolated channels. The environment is interpreted to change from small isolated transverse channels within well drained floodplains to poorer flood plain drainage and deeper more established channels as a result of an increase in seasonal rains. The Ms to Us gravel deposit transport is restricted to within 20 km of the topographic mountain front (DeCelles et al., 1998b). This is observed in the Dhan Khola formation (Us) where the lithology and thickness vary greatly from north to south (Regumi et al., 2011). This thickness variation in the Us may also be attributed to active thrusting in the Siwalik Group at the time of deposition.

3. GEOLOGY OF THE DANG VALLEY AREA

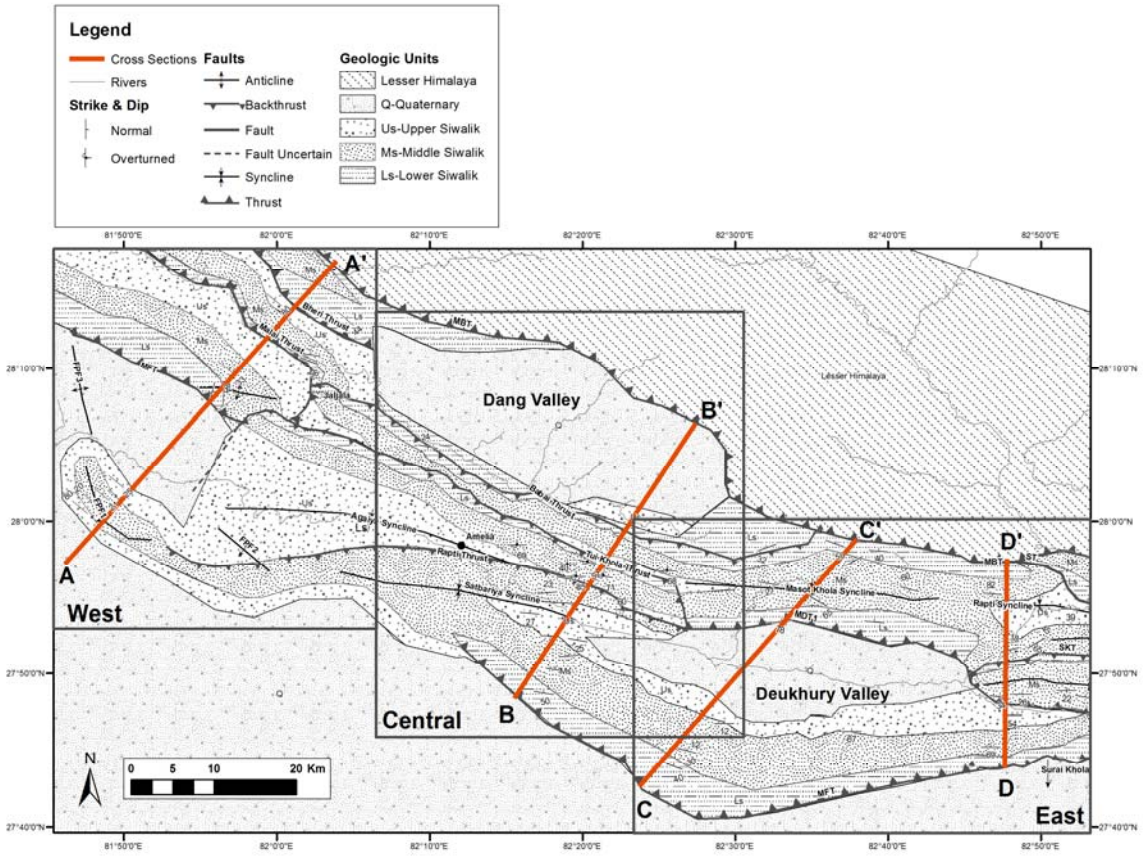

Figure 7: Sections of study area defined by structural styles. Cross sections are outlined within their associated regions.

Rocks within the Dang Valley to Surai Khola Area were mapped by the Department of Mines and Geology Nepal, Mugnier et al. (1999), Nakayama and Ulak (1999), and Regumi et al. (2011). The study area consists of 3 different regions, the western, central, and eastern sections (Figure 7), each with characteristic structural styles.

3.1. Western Section

In the western section (Figure 8), north-dipping beds of Ls, Ms, and Us are present between south-verging thrusts that parallel the thrust front defined by Regumi et

al. (2011) as the Bheri Thrust, Malai Thrust, and the MFT from north to south. The Bheri Thrust, located just south of the MBT, tips out to the east into the Dang Valley under the Quaternary alluvium. The Malai Thrust parallels the thrust front until just south of the Dang Valley where the fault trace turns southward and branches with the Babai Back thrust south of the Dang Valley. The MFT fault underlies the anticline known as the Khairi Khola Anticline (Regumi et al., 2011). The southernmost structure is a fault propagation fold which creates an anticline at the surface which dies out to the west and the east (Mugnier et al., 1999).

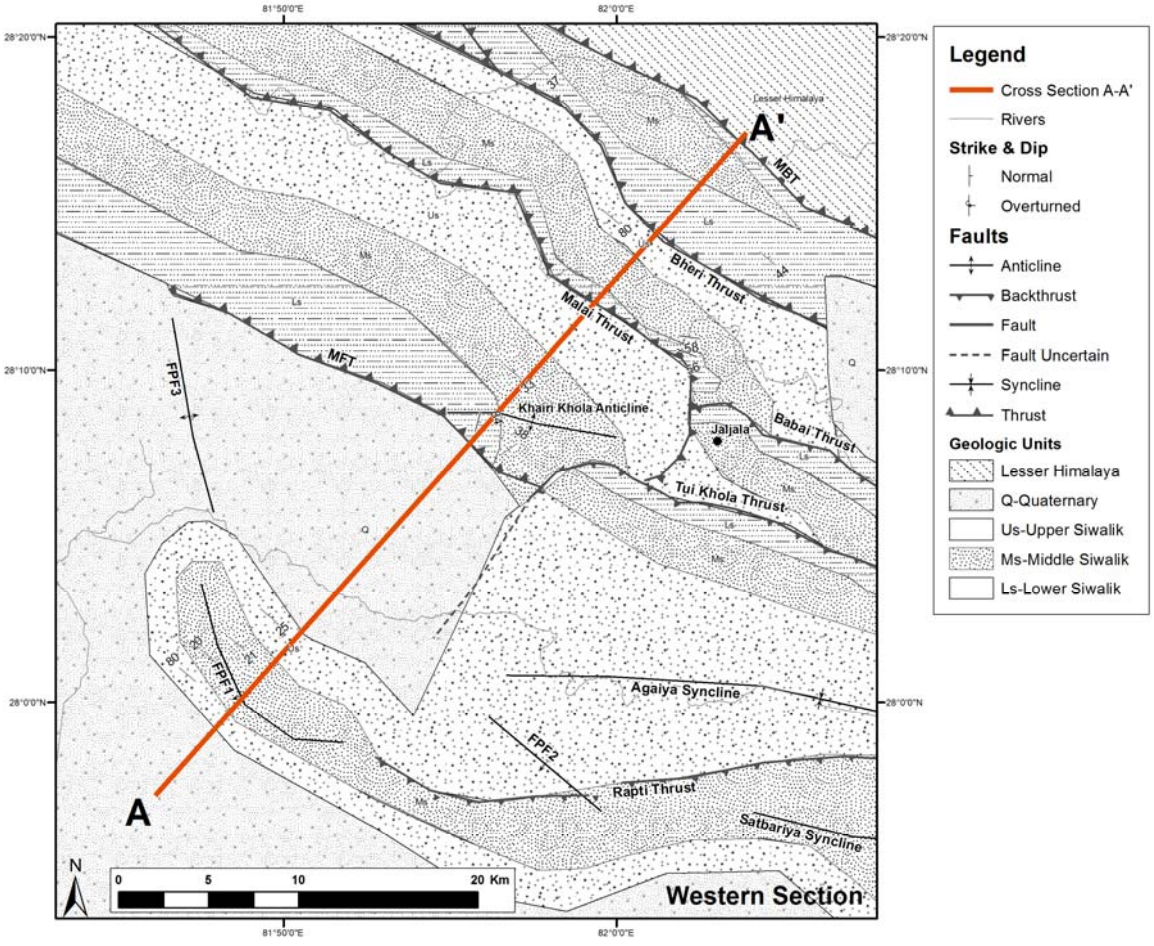

Figure 8: Geologic map of the western section and location of cross section A-A'.

3.2. Central Section

The central section is located south of the Dang Valley (Figure 9) and is characterized by a series of south-dipping back thrusts and synclines. Minor structures found in the Dang and Deukhury Valleys consist of small scale folds, faults and joints. The Dang Valley is relatively flat and filled with Quaternary alluvium. The valley is bounded on all sides by multiple thrusts. To the north, the Dang Valley is bound by the MBT, and to the south, the Babai back thrust, Tui Khola back thrust, and Rapti back thrust (Regumi et al., 2011).

The Babai back thrust sheet is composed of the Ls, Ms, and Us members of the Siwalik group except south of the central Dang Valley where the Us section has been cut by the Tui Khola back thrust, and beds are locally overturned. This overturned is 50 km long and 4 km wide (Regumi et al., 2011).

The Babai back thrust parallels the stratigraphy except near Jaljala (Figure 8), at its western extent, where the fault obliquely cuts the entire section creating a ramp that runs perpendicular to the thrust front before branching with the Tui Khola Back thrust to the south. The fault bounds the Khairi Khola Anticline to the west of the ramp (Regumi et al., 2011).

The Tui Khola back thrust parallels the stratigraphy and the MBT in a northwest to southeast orientation. At the western extent of the back thrust, the fault forms a ramp oriented southward and obliquely cutting the hanging wall stratigraphy (Figure 8). To the west of the ramp is the Khairi Khola Anticline. To the south, the dips shallow forming the Agaiya syncline before reaching the Rapti back thrust. In the eastern section (Figure 9) the thrust obliquely cuts the Siwaliks when the faults orientation is perpendicular to the

thrust front before branching with the Rapti back thrust. This creates a ramp with the Masot Khola Syncline in the footwall (Regumi et al., 2011).

The Rapti back thrust obliquely cuts the Agaiya Syncline (Figure 9). To the west the syncline is well exposed, but to the east, the thrust obliquely cuts the Us section and only the Ms overturned beds in the Tui Khola back thrust are present in the hanging wall. The dips within the Tui Khola back thrust shallow to the south forming the Satbariya syncline (Regumi et al., 2011). The southern extent of the syncline is bounded by the MFT where Ls, Ms, and Us are exposed in the central and eastern portion of the syncline. The syncline is filled with Quaternary alluvium to the west and is part of a larger structure known as the Deukhury Valley.

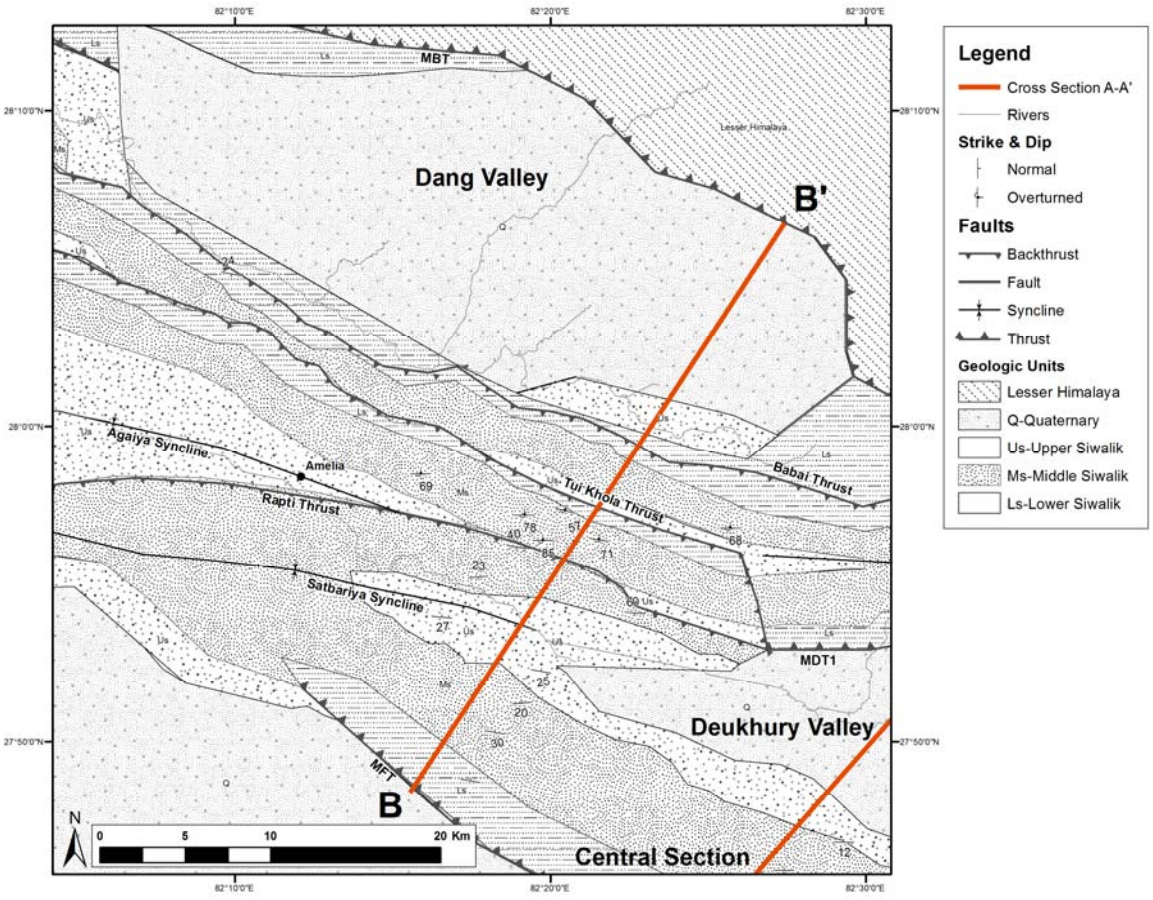

Figure 9: Geologic map of the central section and location of cross section B-B'.

3.3. Eastern Section

The eastern section (Figure 10) is located in the Surai Khola area and exposes south-verging and north-verging thrusts bounding multiple synclines. The Babai back thrust, (Regumi et al., 2011) also known as the Internal Decollement Thrust (ID), (Mugnier et al., 1999) branches with the MBT on the eastern edge of the Dang Valley forming the northern boundary of Masot Khola syncline. The limbs of the syncline consist of Ls and Ms, with Us in the core. The southern boundary of the syncline is the Main Dun Thrust 1 (MDT1) defined by Mugnier et al. (1999). The north-dipping thrust

branches with the Rapti back thrust to the west and forms the southern boundary of the Masot Khola syncline and the northern boundary of the Deukhury Valley. The MFT bounds the Deukhury Valley to the south. Outcrops of the Siwalik Group dip toward the center of the Deukhury valley. The MFT parallels the strata in the thrust sheet and contains outcrops of Ls near the fault, Ms, and then Us in the center of the valley.

Farther to the east the MDT1 branches with the Silling Khola Thrust (SKT) to the north (Mugnier et al., 1999) forming a small syncline. The north-dipping MDT1 forms the southern boundary of the syncline and the south-dipping SKT forms the northern boundary. Very little Ls is exposed on either flank of the syncline and Ms and Us are exposed in the core. The Rapti syncline, located to the north of the SKT and south of the MBT, contains the entire Siwalik section on the northern limb. The southern limb is missing the Ls Formation. The Sit Khola Thust (ST) is located north and east of the Rapti Syncline and contains only Ls and Ms south of the MBT (Nakayama and Ulak, 1999). The ST is interpreted to dip to the south and branches with the MBT to the north.

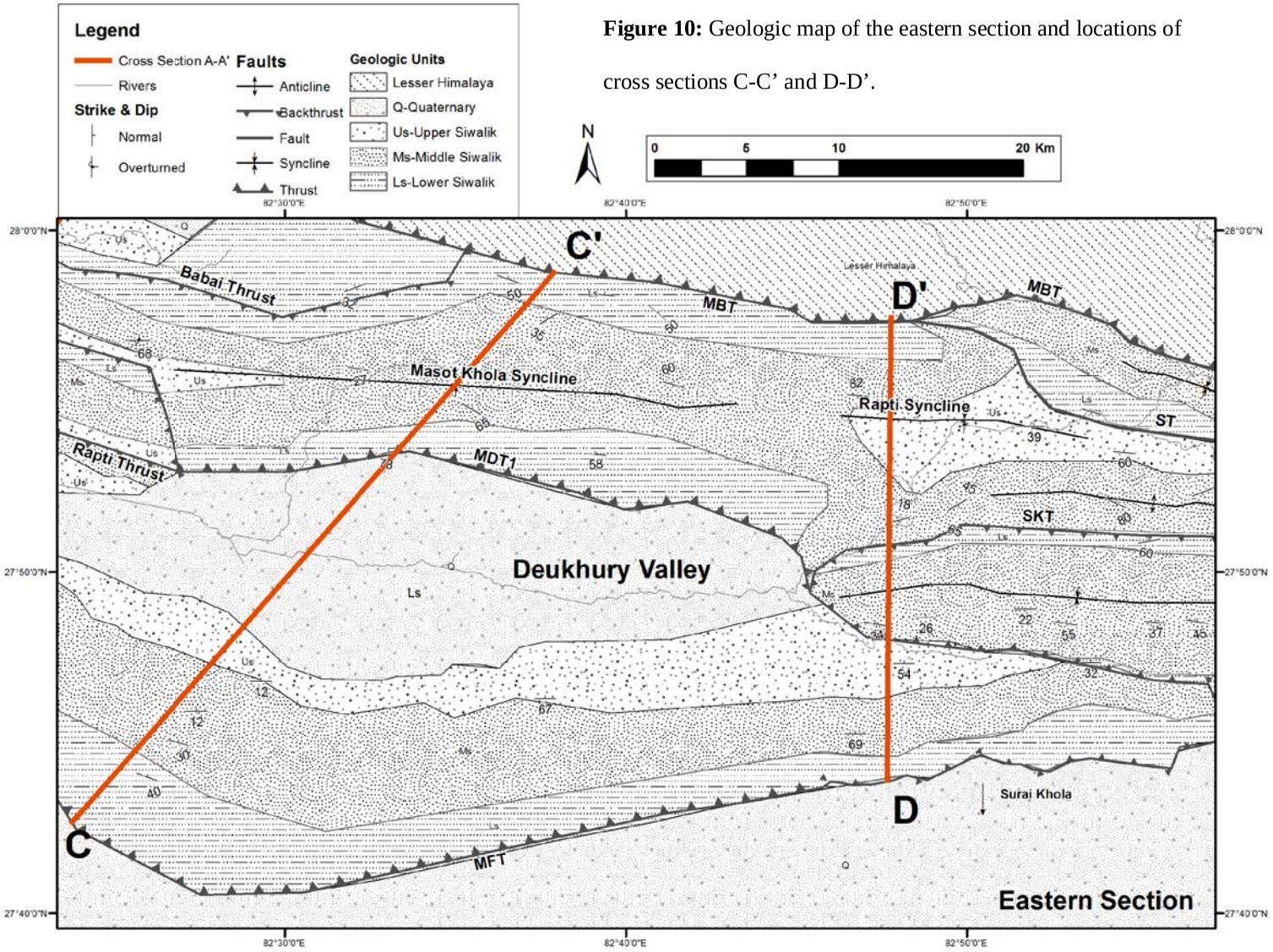

Figure 10: Geologic map of the eastern section and locations of cross sections C-C' and D-D'.

3.4. Cross Sections

Four cross sections were constructed across the study area to illustrate changes in structural style from west to east. Section A-A' is in the western section, section B-B' is in the central section, and sections C-C' and D-D' are in the eastern section (Figures 7, 8, 9, and 10). Midland Valley Move and 2DMove was used to aid in interpretations of the fault geometry and structural relationships at depth. Details of how this was conducted are described in section 5, Kinematic Modeling.

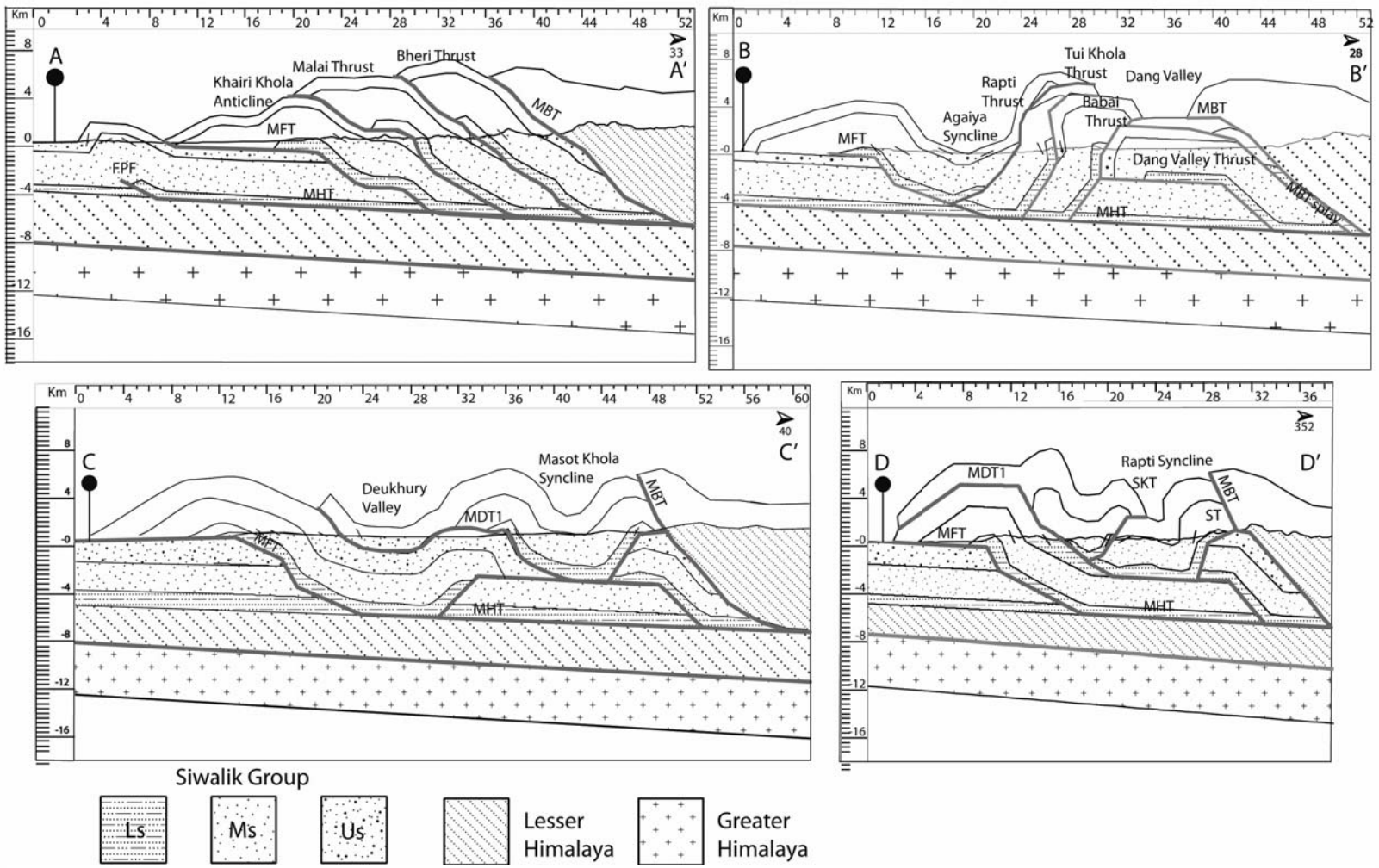

Figure 11: Cross Sections A, B, C, and D constructed using 2DMove. Cross sections show changes in structural styles from west to east across the study area. See list of Abbreviations.

3.4.1. *Cross Section A-A'*

In cross section A-A', (Figure 11) the Siwalik group crops out to the south of the Lesser Himalayan rocks in the MBT sheet. The Ls, Ms, and Us Members are exposed in all thrust sheets. Thickness data were taken from measured stratigraphic sections from the Ameliya region (Regumi et al., 2011). The thicknesses for Ls, Ms, and Us are 800 m, 2900 m, and 800 m, respectively.

The Bheri Thrust, Malai Thrust, and MFT are interpreted as north-dipping imbricates. The MFT is structurally beneath the Khairi Khola anticline. A hanging wall flat is interpreted within the Ms Formation. The position and location of the flat explains the geometry of the rock units as well as the Khairi Khola anticline. The anticline to the south is interpreted as a fault propagation fold (Mugnier et al., 1999) that soles into the same detachment as the imbricate faults.

All faults sole into the same detachment surface located at a depth of approximately 7 km near the MBT and 5 km near the fault propagation fold in the south with a dip of 3 degrees north. Estimates of depth and slope of the detachment were guided by studies based on seismicity in western Nepal (Pandey et al., 1999) as well as cross sections constructed in western Nepal (Robinson, 2008). Forward modeling is used to interpret geometries of structures observed at the surface into the subsurface. The geometries generated in these models also guided the depth to detachment.

3.4.2. *Cross Section B-B'*

The MBT bounds the Siwalik Group to the north (Figure 11). Thicknesses are the same as used in cross section A-A'. The Siwalik Group are deformed by a series of faults consisting of south-directed thrusts and north-directed back thrusts. In the north, a splay of the MBT is interpreted to displace Ls to the surface. Ls is exposed as a lens paralleling the MBT in the northern margin of the Dang Valley. To the south, a horizontal thrust sheet lies structurally above a footwall ramp involving Ls and Ms forming the extent of the Dang Valley. The southern margin of the Dang Valley corresponds to the southern extent of this sub-horizontal thrust sheet.

The Babai back thrust, Tui Khola back thrust, and Rapti back thrust are south-dipping imbricate back thrusts that emplace Ls and Ms over the south margin of the Dang Valley thrust sheet. The Us Formation of the Tui Khola back thrust sheet is cut by the Rapti back thrust. Beneath the back thrusts, the MFT is a shallow dipping footwall ramp, affecting the detachment level of the Tui Khola back thrust and the Rapti back thrust. The Rapti back thrust branches on the footwall ramp of the MFT fault creating a syncline in the Deukhury Valley. All faults sole into the same detachment level. Near the MBT the depth to detachment is 7 km and beneath the MFT ramp the depth is 5 km. The slope of the detachment is approximately 3 degrees north in this region.

3.4.3. *Cross Section C-C'*

Cross section C-C' (Figure 11) is located in the eastern section of the study area. The thickness of the Ms and Us Members is taken from the study completed by Nakayama and Ulak (1999) in the Surai Khola area. The thickness of Ls is taken from the stratigraphy from the Ameliya region (Regumi et al., 2011) because the entire section is not exposed in the Surai Khola area. The thicknesses used in this cross section for Ls, Ms, and Us are 1850 m, 2500 m, and 800 m, respectively.

The MBT bounds the Siwalik Group to the north. South of the MBT, a footwall ramp in the Ls and Ms Members uplifts a thrust sheet containing Ls, Ms, and Us in the hanging wall of the MDT1. This hanging wall is cut by a south-dipping back thrust which creates beds dipping to the south. The MDT1 fault has been uplifted to the south of the back thrust by a blind back thrust which creates a wedge propping up the MDT1 rocks. The resulting structure is a "pop-up" syncline or piggy back basin which soles into the shallow detachment created by the MDT1 fault. The MFT displaces Ls, Ms, and Us to the south of the pop-up structure along a footwall ramp. The rocks in the MFT sheet are north-dipping due to displacement over a foot wall ramp and the rocks to the north are south-dipping due to movement along a blind back thrust that creates a wedge. This geometry creates a syncline in the Deukhury Valley with the southern limb exposed at the surface and the northern limb hidden beneath the MDT1 and Quaternary alluvium from the Rapti River.

Faults in this section sole into 2 main detachments. The first detachment is at the same structural level as the adjacent cross sections at the base of the Siwalik Group. The depth to detachment near the MBT is 8 km and the depth at the base of the MFT footwall

ramp is 6 km. The slope of the detachment is approximately 3 degrees. The shallow detachment is located at the top of the Ms section in the hanging wall of the MDT1. The depth to this shallow detachment is approximately 3 km. The back thrust that forms the pop-up structure soles into this detachment. The presence of a secondary detachment is interpreted to have created a weak point for the wedge below the MDT1 to propagate along.

3.4.4. *Cross Section D-D'*

Cross section D-D' (Figure 11) is located in the eastern section of the study area. Thickness data for the Ls, Ms, and Us Members is taken from measured sections completed by Nakayama and Ulak (1999) in the Surai Khola area. Ls thickness data was taken from measured stratigraphic sections from the Ameliya region (Regumi et al., 2011) because the entire Ls section is not exposed in the Surai Khola area. The thicknesses used in this cross section for Ls, Ms, and Us are 1850 m, 2500 m, and 800 m, respectively.

The MBT bounds the Siwalik Group to the north and contains deformed rocks of the Lesser Himalayan sequence. South of the MBT, a horizontal thrust sheet lies structurally above a footwall ramp involving Ls and Ms. The MDT1 sheet contains north-dipping Ls, Ms, and Us in the hanging wall. Two back thrust faults (SKT and ST), branch with the north-dipping MDT1, uplifting rocks to the north creating southward dipping strata. The resulting structures in the hanging wall of the MDT1 are pop-up synclines.

Two main detachment levels are observed in this cross section. The first detachment is at the same structural level as the adjacent cross sections at the base of the

Siwalik Group. The depth to detachment near the MBT is 7 km and the depth at the base of the MFT footwall ramp is 6 km. The slope of the detachment is approximately 3 degrees North in this region. The second detachment is located at the top of the Ms section in the hanging wall of the MDT1. The depth to this detachment is approximately 3 km. The back thrusts that form the pop-up structures sole into this detachment surface.

4. KINEMATIC MODELING

Forward modeling was performed on each cross section in order to better understand the kinematics and geometry of faulting in the study area. The cross-section geometry and kinematics of each model was modified until structures in the subsurface produced the observed attitudes and map patterns of the Siwalik Group. Forward modeling aided in the interpretation of these complex structures.

Data from the basemap generated in ArcGIS was integrated into Move with a 90 m digital elevation model (DEM) from the United States Geological Survey (USGS) to generate the profiles for interpretation in the cross section. Cross sections were generating using Midland Valley 2DMove. Forward modeling techniques were used in 2DMove to deform strata along a fault plane using the fault bend fold and fault propagation fold methods when appropriate. The fault planes and displacement magnitudes were adjusted until the resulting deformation matched the geologic contacts and strike and dip data collected from the geologic maps.

4.1. Forward Model A-A’

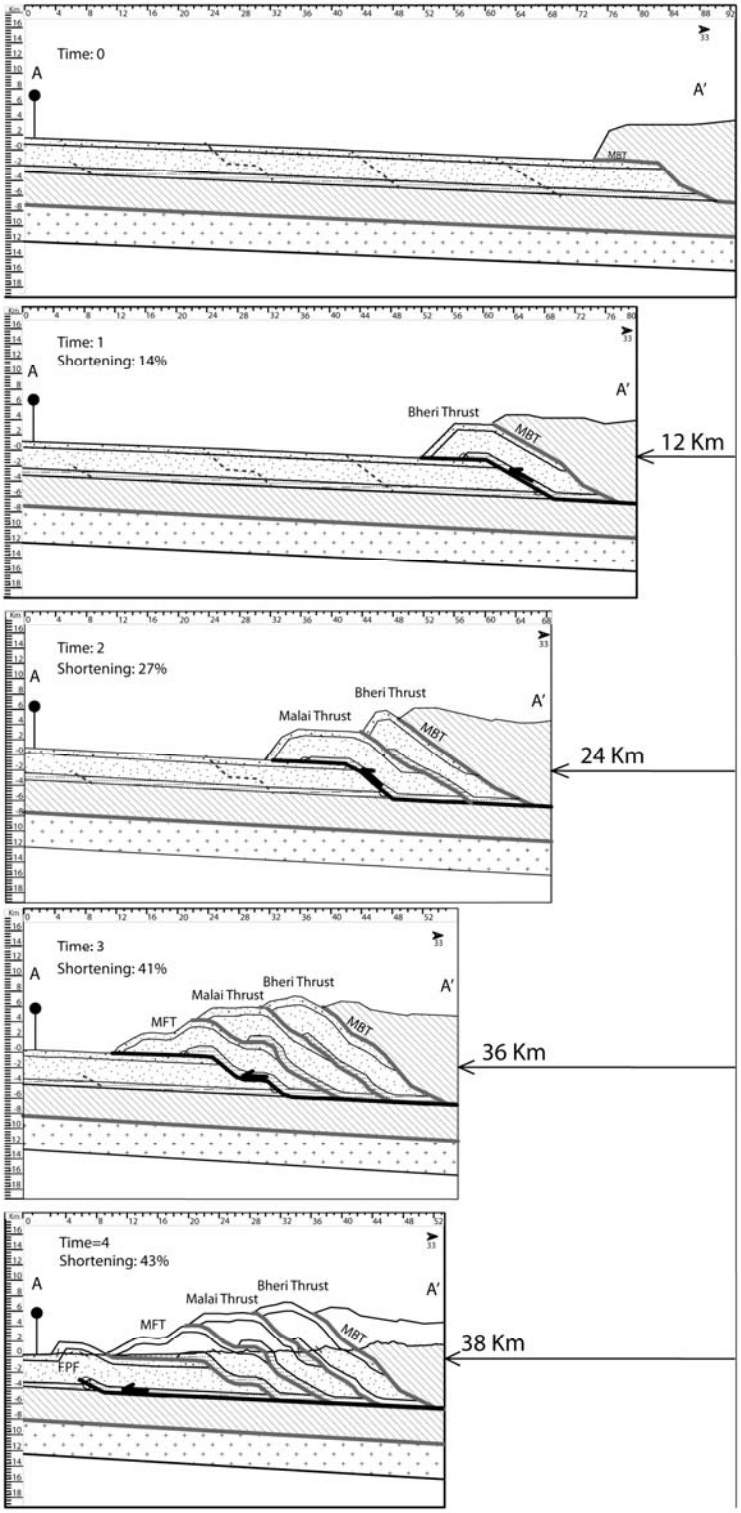

Figure 12: Kinematic Model of Cross Section A-A’. Time steps 1 through 4 were constructed using 2DMove. Magnitude of shortening is shown with arrows from right to left. Dashed lines are future fault locations. Bold faults represents faults active at that time step. Arrow illustrates shortening direction. Last time step represents present day conditions with topographic profile showing erosion.

4.1.1. *Kinematics*

The initial condition presented in the model (Figure 12) includes sub-horizontal Ls, Ms, and Us rocks to the south of the north-dipping MBT. At time 1, the foreland propagating Bheri thrust cuts the entire Siwalik section along a footwall ramp and uplifts the Lesser Himalayan rocks of the MBT sheet. At time 2, to the south, the Malai Thrust cuts the entire Siwalik section along a footwall ramp uplifting and further deforming the Bheri Thrust sheet. At time 3, the MFT propagates south of the Malai Thrust along a flat to ramp to flat to ramp to flat fault plane. The flat within Ms creates the geometry of the thrust sheet needed to create the khairi Khola anticline at the surface. At time 4, the imbricate thrusts slide southward along the detachment creating a fault propagation fold to the south. The sequence of these structures based on kinematic modeling is reasonable based on other studies completed in the Himalayan Mountains. The fault is modeled to be foreland propagating (Robinson et al., 2008) as the thrust wedge deformed sequentially to the south along the MHT. (Hodges et al., 2001; Larson et al., 2010).

4.1.2. *Shortening*

The percent shortening for each time step is calculated using the initial condition and the cumulative amount of shortening that occurred as each thrust sheet is displaced (Figure 12). The initial condition is 89 km from the MBT to the pin. The cumulative magnitude of shortening at time one is 12 km (14%), at time two is 24 km (27%), at time three is 36 km (41%), and at time four is 38 km (43%).

4.2. Forward Model B-B’

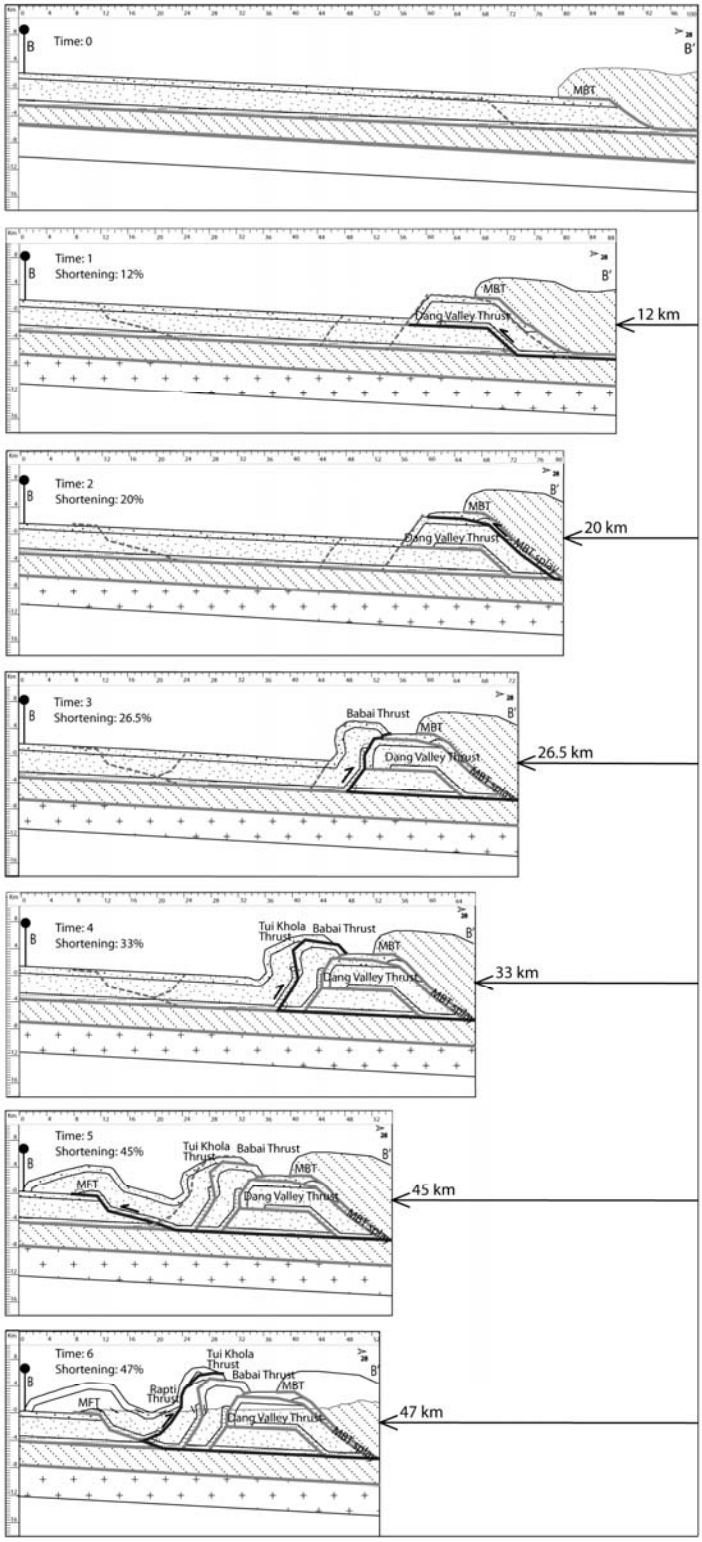

Figure 13: Kinematic Model of Cross Section B-B’. Time steps 1 through 6 were constructed using 2DMove. Magnitude of shortening is shown with arrows from right to left. Dashed lines are future fault locations. Bold faults represents faults active at that time step. Arrow illustrates shortening direction. Last time step represents present day conditions with topographic profile showing erosion.

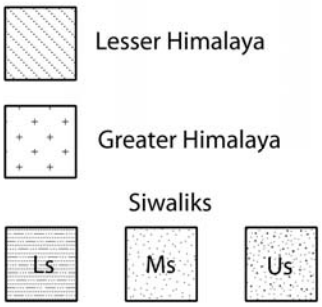

4.2.1. *Kinematics*

The initial condition presented in the model (Figure 13) includes sub-horizontal Ls, Ms, and Us rocks to the south of the north-dipping MBT. At time 1, the foreland propagating thrust cuts the Ls and Ms Members of the Siwalik section along a footwall ramp and uplifts the Lesser Himalayan rocks of the MBT. At time 2, a splay of the MBT displaces Ls currently under the Quaternary alluvium along the northern margin of the Dang Valley. At time 3, the south-dipping Babai back thrust uplifts the rocks of the Siwalik group overturning the hanging wall. At time 4, another south-dipping back thrust known as the Tui Khola Thrust uplifts the entire Siwalik section structurally above the hanging wall of the Babai back thrust. At time 5, the MFT displaces the Siwalik section to the south along a footwall ramp. Then at time 6, the Rapti back thrust forms in the hanging wall of the MFT above the Ls Formation along the footwall ramp. This model involves a foreland propagating system composed of a series of south-verging thrusts and multiple in and out of sequence north verging back thrusts.

4.2.2. *Shortening*

The percent shortening for each time step is calculated using the initial condition and the cumulative amount of shortening that occurred as each thrust sheet is displaced (Figure 13). The initial condition is 100 km from the MBT to the pin. The cumulative magnitude of shortening at time one is 12 km (12%), at time two is 20 km (20%), at time three is 26.5 km (26.5%), and at time four is 33 km (33%), at time five is 45 km (45%), and at time six is 47 km (47%).

4.3. Forward Model C-C’

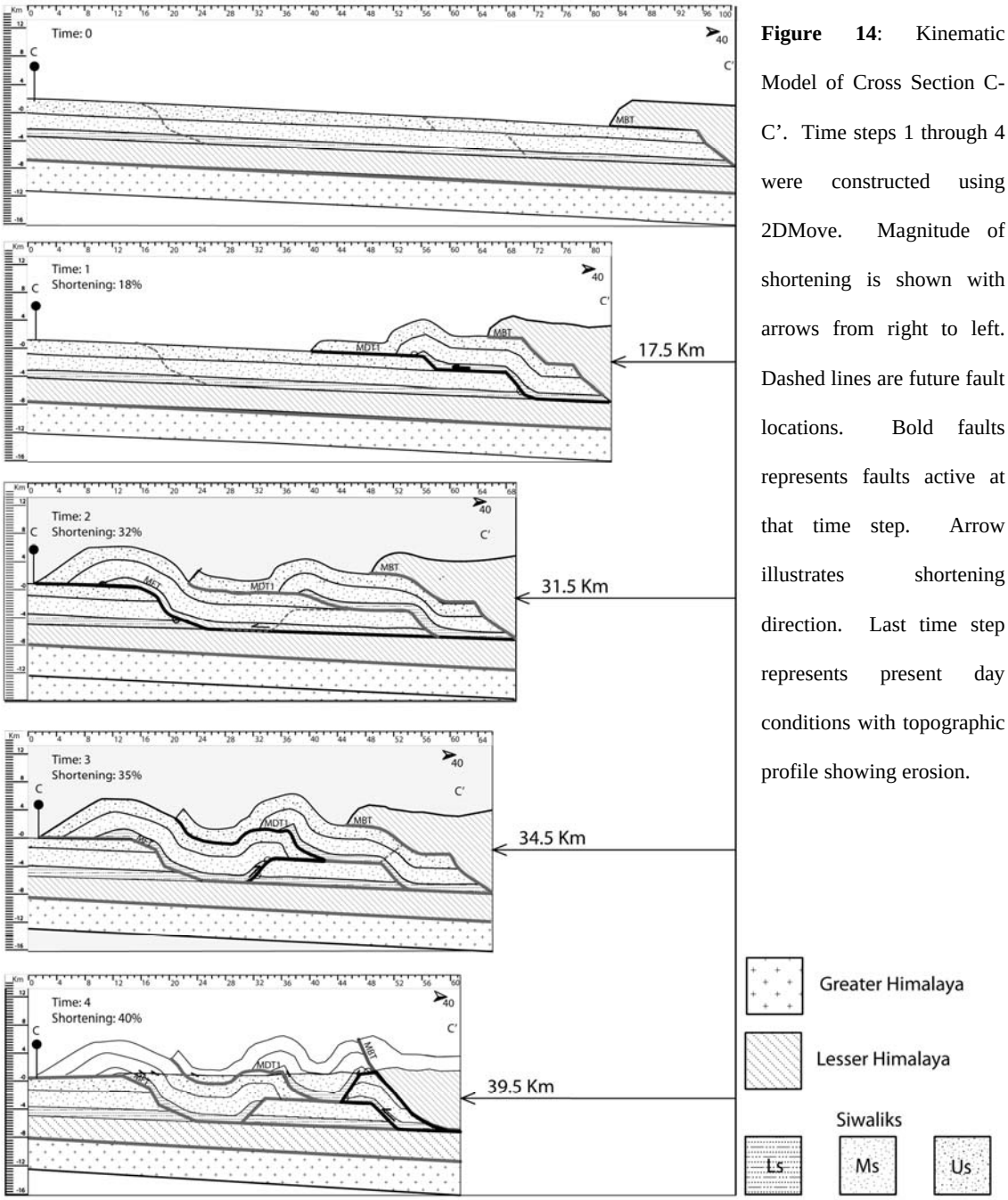

Figure 14: Kinematic Model of Cross Section C-C’. Time steps 1 through 4 were constructed using 2DMove. Magnitude of shortening is shown with arrows from right to left. Dashed lines are future fault locations. Bold faults represents faults active at that time step. Arrow illustrates shortening direction. Last time step represents present day conditions with topographic profile showing erosion.

4.3.1. *Kinematics*

The initial condition presented in the model (Figure 14) includes sub-horizontal Ls, Ms, and Us rocks to the south of the north-dipping MBT. At time 1, the north-dipping MDT1 cuts the Ls and Ms Members along a foot wall ramp. The hanging wall then moves along a flat before cutting the Us Formation with a foot wall ramp to the south. The Displacement along the MDT1 uplifts the Siwalik section and the Lesser Himalayan rocks of the MBT. At time 2, the MFT propagates to the south along a footwall ramp uplifting the entire Siwalik section. At time 3, a blind, south-dipping, back thrust creates a wedge propping up the MDT1 hanging wall, creating the southern limb of the syncline. At time 4, another blind, south-dipping, back thrust is created just south of the MBT as a wedge develops along the MDT1 which uplifts the northern limb of the syncline. This model initially develops as a foreland propagating system of imbricate faults followed by out of sequence blind back thrusts forming along a shallow detachment (MDT1 fault plane).

4.3.2. *Shortening*

The percent shortening for each time step is calculated using the initial condition and the cumulative amount of shortening that occurred as each thrust sheet is displaced (Figure 14). The initial condition is 100 km from the MBT to the pin. The cumulative magnitude of shortening at time one is 17.5 km (18%), at time two is 31.5 km (32%), at time three is 34.5 km (35%), and at time four is 39.5 km (40%).

4.4. Forward Model D-D''

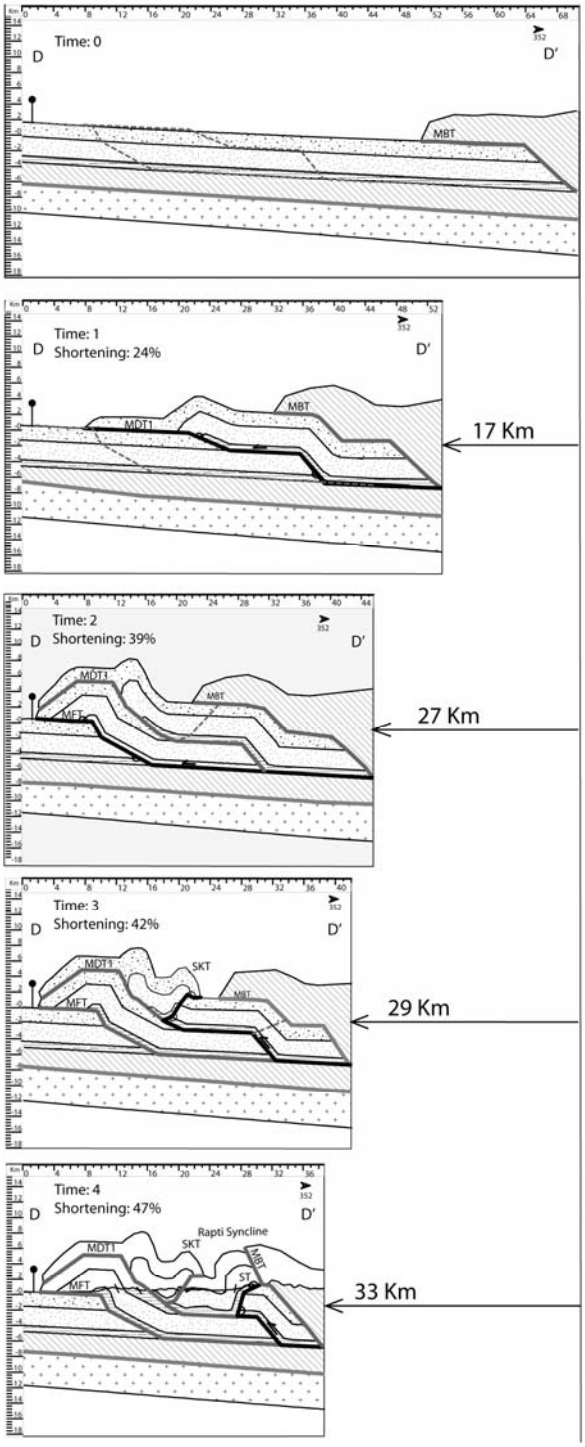

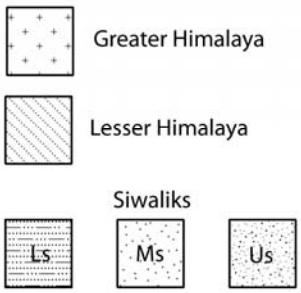

Figure 15: Kinematic Model of Cross Section D-D'. Time steps 1 through 4 were constructed using 2DMove. Magnitude of shortening is shown with arrows from right to left. Dashed lines are future fault locations. Bold faults represents faults active at that time step. Arrow illustrates shortening direction. Last time step represents present day conditions with topographic profile showing erosion.

4.4.1. *Kinematics*

The initial condition presented in the model (Figure 15) includes sub-horizontal Ls, Ms, and Us rocks to the south of the north-dipping MBT. At time 1, the north-dipping MDT1 thrust cuts the Ls and Ms Members along a foot wall ramp. The hanging wall then moves along a flat before cutting the Us Formation with a foot wall ramp to the south. Displacement along the MDT1 uplifts the Siwalik section and the Lesser Himalayan rocks of the MBT. At time 2, The MDT1 fault is uplifted by the propagation of the MFT along a footwall ramp to the south. The uplift from the MFT folds the beds of the MDT1 creating north-dipping beds. The MFT uplift and the foreland propagation of the thrust wedge form the southern margin of pop-up structures or piggy-back basins in the hanging wall of the MDT1 sheet. At time 3, the SKT back thrust creates the northern limb of the syncline. At time four, a wedge forms along the MDT1 uplifting rocks along the ST fault creating the larger Rapti Syncline. The SKT and the ST synclines share the same southern limb created by the uplift of the MFT. The model illustrates a foreland propagating system of imbricate faults with 2 piggyback basins forming as a result of out of sequence back thrusting along the MDT1 shallow detachment surface.

4.4.2. *Shortening*

The percent shortening for each time step is calculated using the initial condition and the cumulative amount of shortening that occurred as each thrust sheet is displaced (Figure 15). The initial condition is 70 km from the MBT to the pin. The cumulative magnitude of shortening at time one is 17.5 km (24%), at time two is 27 km (39%), at time three is 29 km (42%), and at time four is 33 km (47%).

5. INTERPRETATION AND DISCUSSION

5.1. Along Strike Variations of Structural Style

The three sections across the Subhimalayan Zone show pronounced differences in structural style. In the western section, north-dipping imbricate thrusts and fault propagation folds are present. In the central section, multiple south-dipping back thrusts create a topographic high to the south of the Dang Valley and north of the MFT. In the eastern section, imbricate thrusts are deformed by a series of south-dipping back thrusts along a shallow detachment creating composite pop-up structures. The MFT has a flat ramp flat geometry at the toe of the thrust belt in the central and eastern sections that forms a hanging wall syncline. There are abrupt changes in structural style observed at the boundaries between sections.

5.1.1. *West Dang Transfer Zone*

Between the western and central sections lies the West Dang Transfer Zone (WDTZ) (Mugnier et al., 1999). The zone marks the change from foreland propagating imbricate thrusts to multiple back thrusts south of the Dang Valley and synclines. Transfer zones are interpreted by Mugnier et al. (1999) to explain the variation in structural style in the Dang Valley area. The WDTZ (Figure 16) consists of strike-slip faults and reverse faults which may be indicative of a change in the detachment level from west to east. A lateral ramp may exist in the area of this transfer zone in order to transfer displacement from one structural level to another.

To the west of the WDTZ the width of the Siwalik structures from the MBT to the MFT averages around 25 km (Mugnier et al., 1999). To the east the faults are south-

dipping back thrusts (Regumi et al., 2011) and the width of the Siwalik structures averages around 40 km (Mugnier et al., 1999.

A topographic low, known as the Dang Valley, forms to the north of the back thrusts and has created a large depocenter known as a Dun which is accumulating Quaternary deposits from the river that flows along the southern margin.

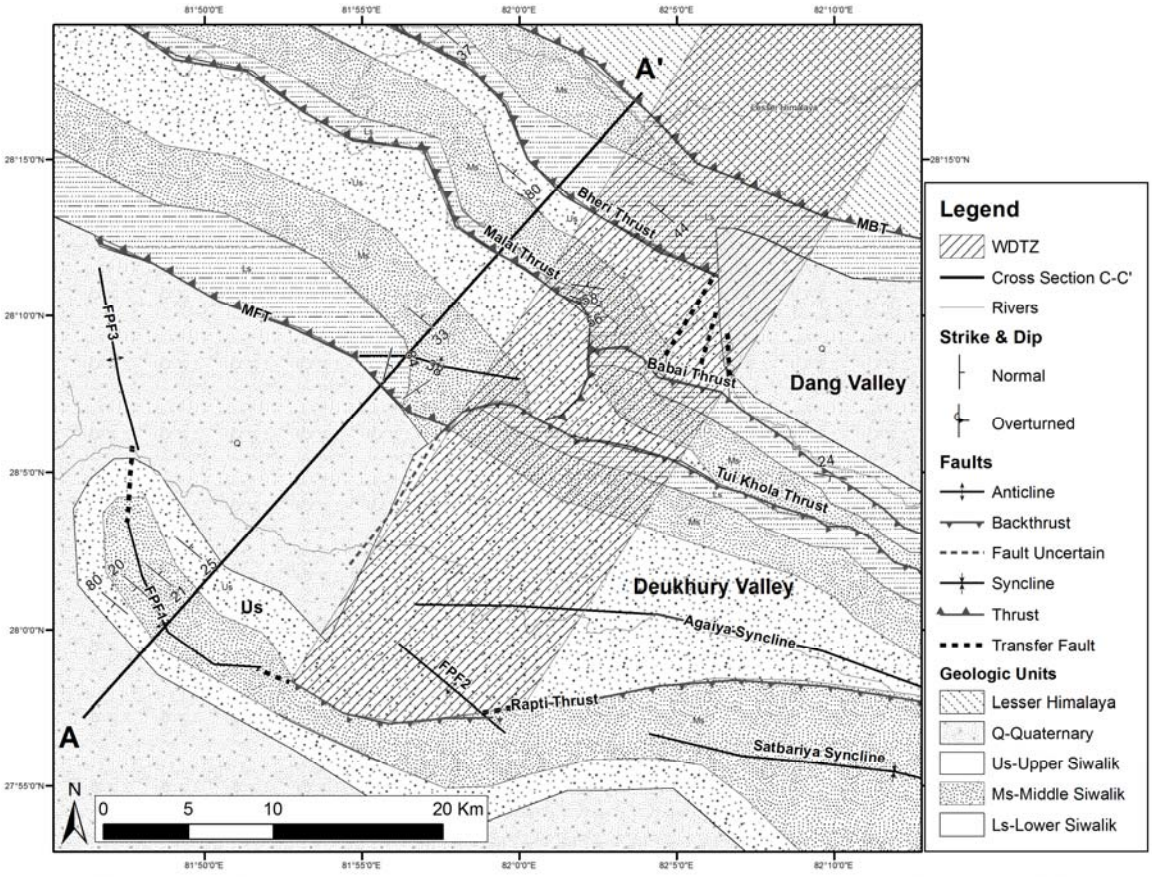

Figure 16: Detailed Geologic Map of West Dang Transfer Zone (WDTZ) (Mugnier et al., 1999; Regumi et al., 2011).

On the western margin of the Dang Valley, multiple dextral strike-slip faults may have formed as a result of dextral torsion of the WDTZ (Mugnier et al., 1999). The

strike-slip faults would have transferred strain from the Bheri Thrust to the Babai back thrust (Figure 16).

The Babai back thrust is oriented north-south within the WDTZ. This fault marks the boundary between north-dipping thrusts to the west and south-dipping back thrusts to the east and may function as a tear fault or a lateral ramp that continues to the south into the western margin of the Agaiya Syncline.

The Rapti back thrust may transfer displacement to fault propagation fold 2 (FPF2) to the west of the Agaiya syncline (Mugnier et al., 1999). Fault propagation fold 1 (FPF1) and fault propagation fold 3 (FPF3) are likely connected to the Rapti back thrust in the subsurface by blind thrusts (Figure 16).

5.1.2. *Masot Khola Transfer Zone*

Between the central and eastern sections an abrupt transition occurs from south-dipping back thrusts to north-dipping thrusts with composite pop-up synclines along a shallow detachment. Figure 17 illustrates the transition from back thrusts to composite pop-up structures through a series of cross sections. The map is divided into 4 fault blocks (Figure 17B). Rocks in these fault blocks were grouped together in order to illustrate the lateral variations in structural character within defined fault blocks. The Lesser Himalaya fault block consists of all rocks to the north of the MBT. The Dang Valley fault block contains all rocks south of the MBT and north of the Babai back thrust. The back thrust to composite pop-up fault block consists of all rocks north of the Rapti back thrust/MDT1 fault trace and south of the Babai back thrust/MBT. The Deukhury Valley fault block contains all rocks to the south of the Rapti back thrust/MDT1 fault trace.

The Babai back thrust defines the southern margin of the Dang Valley section. This fault branches with the MBT in the eastern margin of the Dang Valley. The width of the Dang Valley fault block correlates to the distance between the Babai back thrust and the MBT. The southern extent of the Dang Valley thrust from west to east decreases as the distance between the MBT and the Babai back thrust decreases (Figure17).

The back thrust to pop-up fault block (Figure 17B) is south of the Dang Valley in the west and south of the MBT in the east. To the south of the eastern margin of the Dang Valley, the strike of the Tui Khola back thrust is north-south and branches with the Rapti back thrust marking the lateral ramp referred to herein as the Masot Khola Transfer Zone (MKTZ). This transfer zone separates back thrusts and composite pop-up structures.

The Deukhury Valley fault block is bounded to the north by a linear fault trace comprised of two faults; the south-dipping Rapti back thrust to the west of the MKTZ, and the north-dipping MDT1 fault trace to the east. The southern boundary of the syncline is the arcuate trace of the MFT. The valley is widest south of the MKTZ and converges toward the Rapti back thrust in the west and the MDT1 to the east (Figure 17B).

West of cross section B, (Figure 17A1) the Agaiya Syncline is in the hanging wall of the Tui Khola back thrust sheet and is located north of the Rapti back thrust. The Tui Khola back thrust and the Babai back thrust are at the same structural position in cross section B (Figure 17A2). However, in cross section B, the Agaiya Syncline is cut by the Rapti back thrust which now forms the Satbariya Syncline in the hanging wall.

The back thrust to pop-up fault block detachment surface is at the base of the Siwalik Group west of cross section B (Figure 17A3). At the MKTZ a lateral ramp places the rocks between the Rapti back thrust and the Babai back thrust structurally above a shallow detachment surface. The Rapti back thrust east of the MKTZ is blind and creates a wedge propping up the southern limb of the Masot Khola Syncline exposing the north-dipping MDT1 fault (Figure 17A4). The black dot in Figure 17 marks the position of the northern extent of the Rapti back thrust sheet in the west. The nature of the black dot changes along strike such that, to the east of the MKTZ, the black dot represents the branchline of the blind fault with the MDT1 defining the structural wedge.

The Babai back thrust forms the southern margin of the Dang Valley and branches with the MBT along its eastern margin (Figure 17B). The Babai back thrust is interpreted to be blind east of the Dang Valley forming the northern limb of the Masot Khola Syncline in cross section C (Figure 17A4). The MFT converges with the MDT1 in the eastern portion of the study area (Figure 17B). In cross Section D (Figure 17A5), the blind thrust wedge tips out where the MFT trace is farther to the north decreasing the distance between the MFT and the MDT1. Movement along the MFT places the north-dipping beds above the MFT foot wall ramp closer to the MDT1. The MFT hanging wall uplifts the MDT1 sheet creating the southern limb of 2 pop-up synclines. The northern limb of the smaller syncline is bounded by the SKT back thrust which branches with MDT1 to the west. The ST branches with the MBT and forms the northern limb of the larger syncline and may be a continuation of the blind Babai back thrust exposed at the surface.

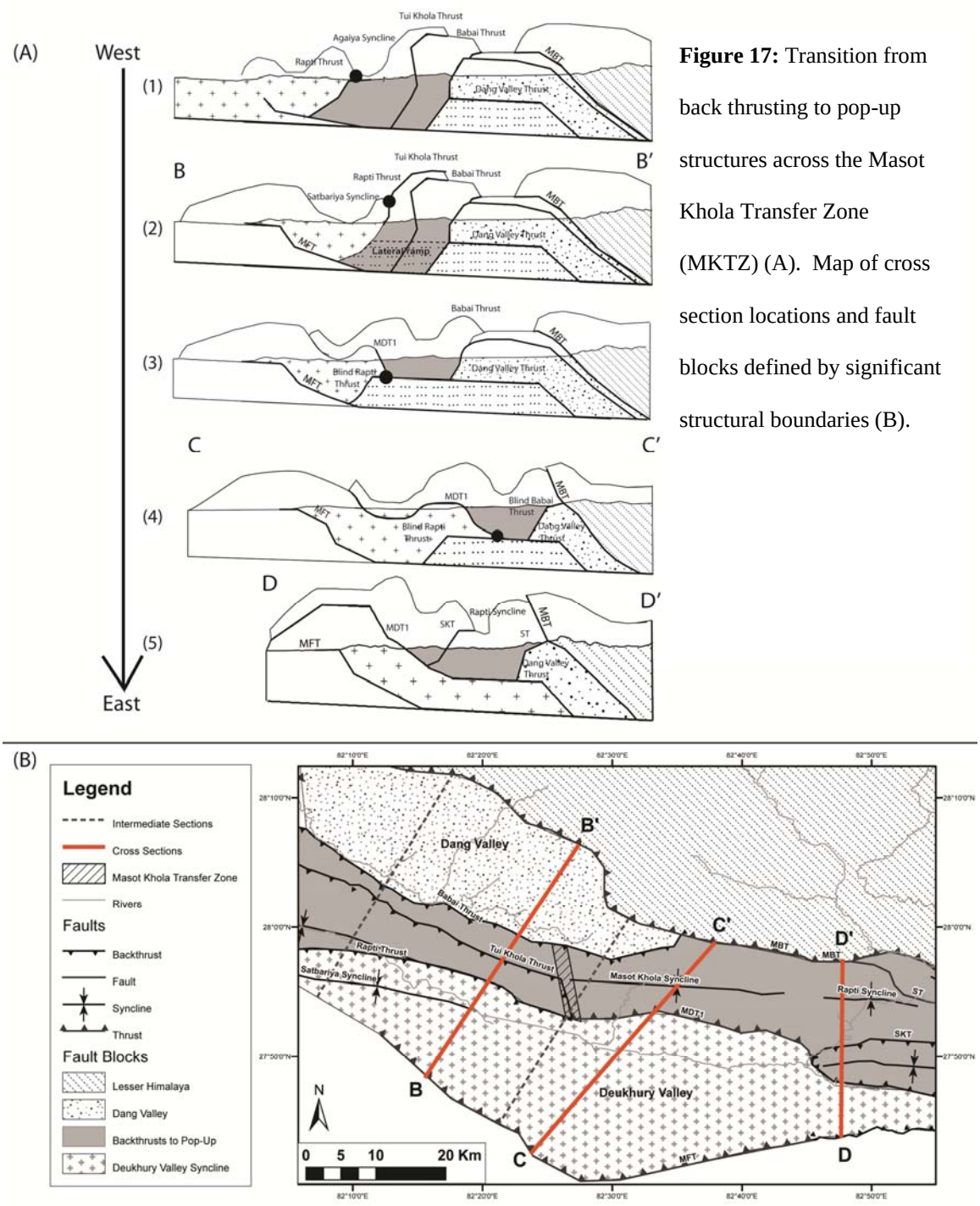

Figure 17: Transition from back thrusting to pop-up structures across the Masot Khola Transfer Zone (MKTZ) (A). Map of cross section locations and fault blocks defined by significant structural boundaries (B).

5.1.3. *Transfer Zone Development*

Models constructed in this study suggest the detachment level deepens across the study area from west to east. Cross section A-A' along strike in the study area (Figure 18), illustrates the interpreted changes in detachment level. The depth to detachment within the MFT sheet in cross section A (Figure 11) is approximately 5 km and the depth to detachment within the Babai back thrust sheet is approximately 5.5 km in cross section B (Figure 11). Therefore, we interpret a 0.5 km high lateral ramp which changes the detachment level from shallow, west of the WDTZ, to deep, east of the WDTZ (Figure 18). The basal detachment level to the west of the MKTZ is approximately 5.5 km deep beneath the Babai back thrust in cross section B (Figure 11) and approximately 6.5 km beneath the hinge of the Masot Khola syncline in cross section C (Figure 11). A lateral ramp drops the basal detachment level by 1 km from west to east across the MKTZ. In addition this lateral ramp branches with a shallow detachment surface at a depth of 3 km (Figure 18).

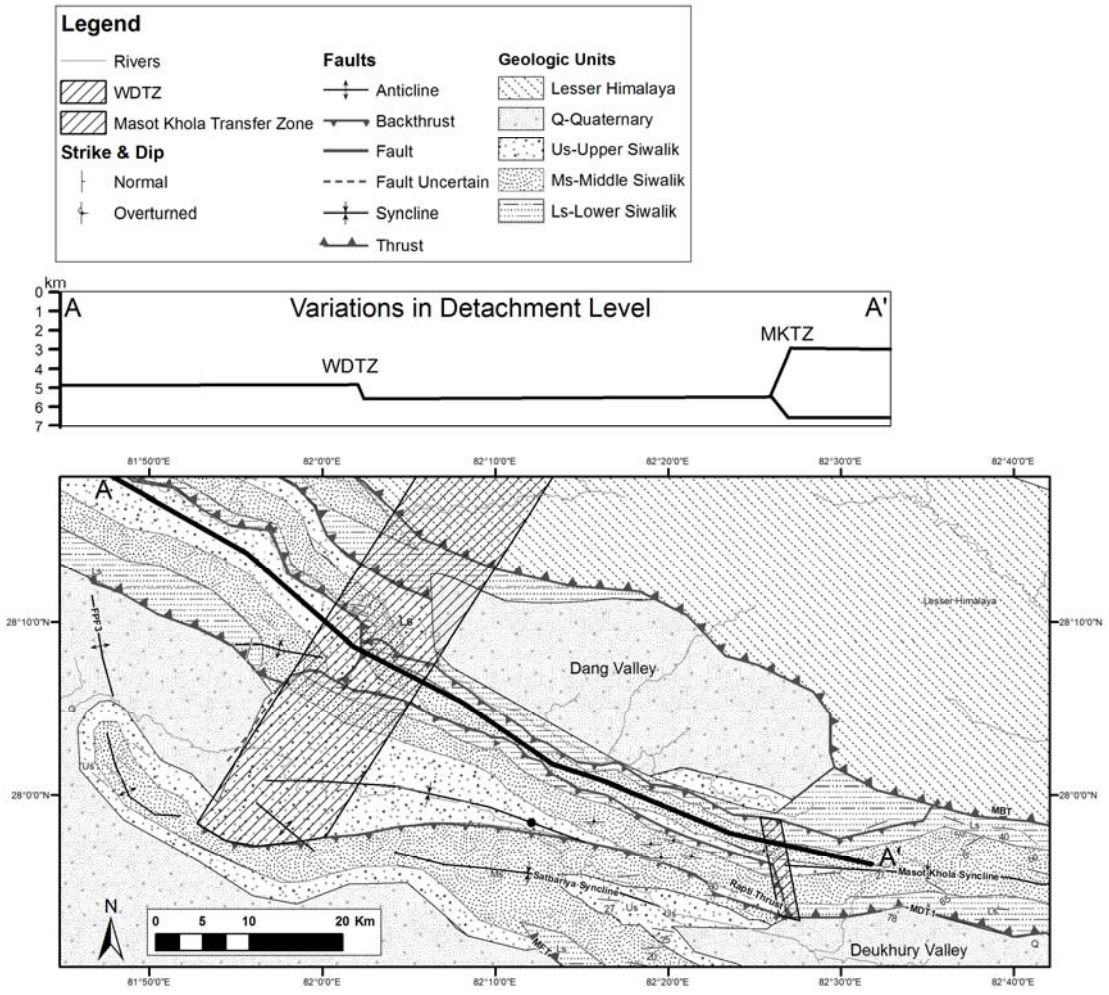

Figure 18: Variations in detachment level. Cross Section A-A' illustrates the modeled change in detachment level across the study area.

The development of transfer zones in thrust belts are thought to be the result of the following parameters according to Calassou et al. (1993): 1) sedimentary thickness variations, 2) backstop steepness, 3) variations in basal friction, and 4) kinked backstop. Stratigraphic thickness variations are observed within the study area and where thickness changes are pronounced, transfer zones could form. Thickness variations across the

transfer zones could be controlled by deep seated basement scarps that change the depth to detachment level (Mugnier et al., 1999; Calassou et al., 1993).

The variations in thickness of the wedge to the north of the MBT as well as the steepness and changes in orientation of the MBT could explain why transfer zones formed in the Subhimlayan Zone. The MBT acts as a backstop by inducing displacement in the foreland along the MHT as the thrust wedge propagates southward. According to Calassou et al. (1993), the backstop steepness and orientation can directly affect transfer zone development.

Generally, the MBT fault trace parallels the thrust wedge. However, east of the WDTZ, north of the Dang Valley, the MBT fault trace is more northward than to the west of the WDTZ (Figure 18). North of MKTZ the MBT orientation is north-south around the eastern margin of the Dang Valley. The orientation to the east of the MKTZ parallels the thrust wedge, however, the fault trace is farther to the south than north of the Dang Valley (Figure 18). The MBT orientation variations observed in map view could be related to changes in the dip of the MBT or offset of the MBT. The condition of the MBT thrust wedge before propagation in the Subhimalayan zone initiated may play a large role in the development of transfer zones and the changes in structural style across them.

5.2. Shortening Estimates and Rates

Balanced cross sections allow me to estimate the minimum amount of shortening between the MFT and the MBT. Mugnier et al. (1999) estimated shortening to be between 17 km to 40 km for sections currently 25 km and 33 km long, respectively. The percent shortening for these sections are 40% and 51%. The difference in shortening

estimates is a result of uncertainties in hanging-wall cutoff locations due to extensive erosion (Mugnier et al., 1999). A minimum shortening rate of 17 mm/yr is calculated based on the shortening estimates assuming deformation began around 2.3 Ma (Mugnier et al., 1999).

Based on the 4 balanced cross sections constructed in this study, the shortening estimates range from 33 km in cross section D to 47 km in cross section B (Table 1). Percent shortening estimates range from 43% in cross section A to 47% in cross sections B and D. These estimates are consistent with those presented by Mugnier et al. (1999).

Cross Sections	Shortening (km)	Shortening (%)	Shortening Rate (mm/yr)	Adjusted Shortening (km)	Adjusted Shortening rate (mm/yr)	Published GPS Derived Shortening Rates (mm/yr)				
						Chen et al. (2004)	Jouanne (1999)	Bilham et al. (1997)	Styron et al. (2011) (arc normal)	Avouac (2003), Lave´ and Avouac (2000)
A	38	43%	17	NA	NA	17-19	19	17.52 ± 2	12	20.4 ± 1*
B	47	47%	20	NA	NA					
C	39.5	40%	17	NA	NA					
D	33	47%	14	23	10					

Table 1: Shortening Data Summary. Table compares magnitudes and rates of shortening from this study with published GPS derived velocity data. Adjusted shortening and shortening rate are normalized to the orientation of plate motion direction. NA- Not adjusted. * Progradation rate along MFT calculated from ages of abandoned terraces versus shortening.

Cross sections A, B, and C are oriented in line with the GPS velocity vectors oriented S40°W near the study area relative to Bangalore, India (Bilham, 1997). Cross section D is oriented perpendicular to structures which are oriented 45 degrees from the GPS vectors. Once the shortening estimate is normalized to the same orientation as the other cross sections, the shortening estimate decreased from 33 km to 23 km. The decrease in shortening magnitude is a result of the obliquity of the corrected orientation to strike.

The unconformity in the Us Formation at 2.3 Ma is interpreted to represents the onset of thrusting in the study area and can be used to estimate shortening rates based on the estimates from our kinematic models. Shortening rates of 17 mm/yr, 20 mm/yr, 17 mm/yr, and 14 mm/yr were calculated for cross sections A, B, C, and D, respectively (Table 1). The normalized shortening rate for cross section D is 10 mm/yr. The rates listed above are consistent with the convergence rates calculated from GPS studies of 17 to 19 mm/yr (Chen et al., 2004; Bilham et al., 1997), 12 mm/yr (Styron et al., 2011), and 19 mm/yr (Jouanne, 1999). Approximately 12 mm/yr of arc-normal shortening was calculated with another 8 mm/yr of arc parallel shear by Styron et al. (2011). The cross sections generated in this study do not account for arc parallel shear, therefore, estimates of shortening represent arc normal shortening.

Our shortening rates, ranging from 14 mm/yr to 20 mm/yr, within the Subhimalayan Zone are comparable to GPS-derived shortening rates in the Nepal Himalaya. This suggests that little shortening is occurring internally within the thrust wedge north of the MBT. However, this is different from what is observed and interpreted in central Nepal where out-of-sequence thrusting has been interpreted at the foot of the High Himalaya approximately 100 km north of the MFT (Wobus et al., 2003; Wobus et al., 2005). Internal deformation is attributed to a four-fold increase in erosion rates which is interpreted to facilitate uplift and exhumation (Wobus et al., 2003; Wobus et al., 2005). The driver for uplift in this region may be a result of high precipitation rates in central Nepal resulting in high denudation rates (Wobus et al., 2005). Alternatively, uplift may be the result of a recent lock-up along a ramp in the MHT (Figure 4). GPS data collected over the last 10 years indicate that the relative motion between the

Gangetic plain and the MFT is minimal and shows that shortening is occuring in a 50 km wide zone south of the High Himalaya and correlates to high seismic activity. However, if shortening is entirely accommodated across the MFT and the MHT as suggested in this study, then strain buildup in the High Himalaya is interpreted to be elastic and alleviated by slip along the MHT/MFT (Lave and Avouac, 2000; Avouac, 2003). Slip along the MFT is not thought to be continuous and is probably the result of multiple seismic events (Lave´ and Avouac, 2000). The potential lock up of the MFT interpreted from GPS velocity data, earthquake locations, and increased denudation rates, may represent moments in geologic time between events as a result of stick-slip behavior along the MHT. The stick-slip behavior of the MHT observed today is indicative of elastic strain buildup that occurs as the thrust wedge propagates to the foreland, however, this study suggests that most of the strain is accommodated along the MFT/MHT in the Subhimalayan Zone once the elastic strain buildup is released.

Another source for comparison of shortening rates is a study conducted in the Subhimalayan Zone, which calculated shortening rates from the age of abandoned terrace deposits (Lave´ and Avouac, 2000; Avouac, 2003) south of Kathmandu Basin. The rate of 20.4 ± 1 mm/yr was calculated and interpreted to represent shortening in the Subhimalayan Zone along the MHT/MFT. This interpretation correlates well with GPS-derived velocities and the results of this study. Similar shortening rates in our study area indicate that shortening may also be focused mainly in the Subhimalayan Zone along the MHT/MFT as observed near Kathmandu Basin.

5.3. Wedge-top Deposition

Uplift of resistant rocks parallel to the thrust front confines transverse rivers creating axial rivers which transport wedge-top sediments from the Lesser Himalaya to the southern margin of duns. Synorogenic sediments are composed of the upper Us Formation and Quaternary surficial deposits. Deposits are identifiable by growth strata patterns including folds and faults and thickness variations as a result of deposition around active structures. Wedge-top deposits typically consist of coarse alluvial and fluvial sediments that accumulate as a result of competing forces of subsidence under the building tectonic load and uplift as a result of wedge propagation (DeCelles and Giles, 1996). Propagation of the fold and thrust belt uplifted and eroded rocks of the Us formation creating a regional unconformity (West and Munthe, 1981; Gautam and Appel, 1984; Harrison et al., 1993; Corvinus, 1998; Mugnier et al., 1999). Pliocene and quaternary sediments deposited above the unconformity are interpreted to be wedge-top deposits.

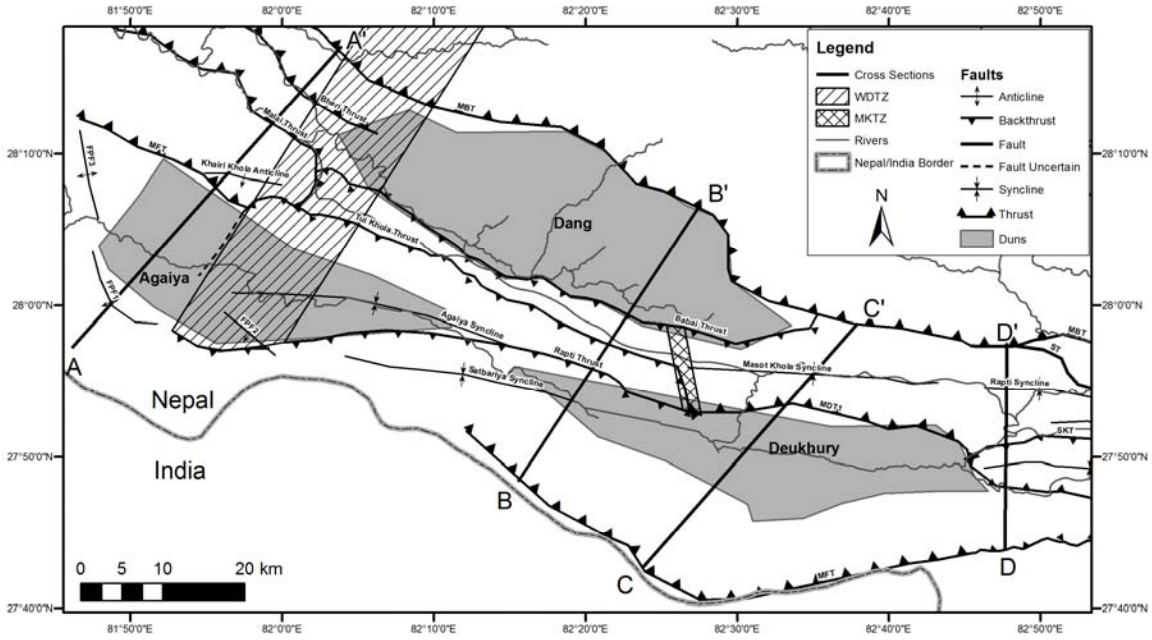

Figure 19: Dun locations in the study area. The WDTZ mark the boundary where changes in structural styles affect wedge-top deposition by forming structures that create duns to the east.

Quaternary alluvium is presently being deposited east of the WDTZ in broad synclinal lows created by the Agaiya syncline and the Satbariya Syncline in the Deukhury Valley (Figure 19). The largest deposits of Quaternary alluvium to the west of the WDTZ are south of the MFT and flank fault propagation folds. The Dang Valley is bounded by steeply dipping back thrusts creating a large, structurally confined basin in which Quaternary alluvium is actively accumulating.

The results of this study suggest there is a relationship between changes in structural style and wedge-top deposition. To the west of the WDTZ, Quaternary alluvial deposits do not accumulate in the narrow axial river channels between the steeply dipping imbricate thrusts; therefore, no duns are observed where this structural style is present

(Figure 19). Conversely, significant deposits of Quaternary alluvium accumulate in the Dang Valley dun to the east, along strike of steeply dipping imbricate thrusts. Therefore, the WDTZ marks an abrupt change not only in structural style as shown in models constructed for cross sections A-A' and B-B' (Figures 12 and 13), but also in Quaternary sedimentation. The latter is evident by the sudden accumulation of wedge-top deposits in the Dang Valley compared to the lack of accumulation of Quaternary deposits to the west. Therefore, where a change in structural style exists, direct evidence of this may be the sudden change in accumualtion of Quaternary deposits.

The Deukhury Valley syncline forms in the hanging wall of the MFT and collects large deposits of Quaternary alluvium along an axial river; however, the composite pop-up structures to the north contain confined axial rivers surrounded by steeply dipping thrust sheets with minimal accumulation of Quaternary alluvium. The narrow composite pop-up synclines form above the shallow detachment level and do not accumulate Quaternary sediments; however, to the south synclines that form along a deeper detachment level are broader and accumulate large deposits of Quaternary alluvium. The depth to detachment level appears to correlate with the amount of Quaternary sediments preserved within the synclines.

6. CONCLUSIONS

This paper provides insight into: the magnitude and rate of shortening accommodated since the Pleistocene in the study area; lateral variations in structural styles; and the effect variations in structural style have on Quaternary alluvial deposition. Kinematic models were constructed to interpret structures in the subsurface in the study area. Three distinct regions were identified based on variations in structural style observed in cross sections. North-dipping imbricate thrust sheets form in the western section, south-dipping back thrusting in the central region, and thrusts sheets containing pop-up structures along a shallow detachment in the eastern section.

Two transfer zones are identified and explain the abrupt changes in structural style. The WDTZ divides north-dipping imbricates in the western section with south-dipping back thrusts south of the Dang Valley in the central section. A lateral ramp in the MKTZ explains the change in structural style from south-dipping back thrusts to piggy back pop-up structures to the east. From west to east, the basal detachment level deepens along the WDTZ ramp, and deepens again along a lateral ramp at the MKTZ. The MKTZ ramp branches with a secondary shallow detachment forming the composite pop-up detachment level.

The average of the shortening estimates calculated in the study area is 44% and the shortening rates range from 14-20 mm/yr based on the initiation of thrusting ca. 2.3 Ma. These estimates of total shortening and shortening rates are consistent with other research in the study area and rates of GPS derived velocities. This implies that in the study area, shortening has been accommodated along a single detachment between the MBT and the MFT since the Pliocene.

Wedge-top deposits are affected by the changes in structural style across the study area. Quaternary deposits collect in broad synclinal structures and valleys bounded by steeply dipping thrusts. Synclines with deeper detachment levels are associated with aerially more extensive wedge-top deposits as opposed to the shallow pop-up structures to the north. The Dang Valley is a structurally confined low that collects wedge-top deposits as a result steeply dipping thrusting at its margins.

7. APPENDIX

7.1. Strike and Dip Data

Study Area Strike and Dip Data				
Strike	Dip	X	Y	Dip Type
95	50	-4944590	4298380	Normal
95	50	-4944368	4296784	Normal
90	44	-4944594	4295648	Normal
280	45	-4947418	4292024	Normal
295	80	-4952833	4296623	Normal
105	45	-4954883	4300347	Normal
270	26	-4962899	4289884	Normal
75	18	-4965109	4293865	Normal
95	82	-4968335	4299054	Normal
310	50	-4980247	4301151	Normal
290	50	-4989085	4301336	Normal
250	32	-4997766	4299620	Normal
275	58	-4982936	4294311	Normal
300	65	-4990221	4295250	Normal
260	78	-4994711	4292600	Normal
105	60	-4978938	4297938	Normal
280	27	-4997010	4296056	Normal
270	67	-4984091	4282960	Normal
270	85	-5020904	4293106	Overturned
270	78	-5022224	4294162	Overturned
285	57	-5019769	4294691	Overturned
100	40	-5022796	4292341	Normal
280	71	-5017441	4293632	Overturned
85	23	-5024955	4290521	Normal
275	27	-5026902	4288383	Normal
270	69	-5028914	4295160	Overturned
270	68	-5009415	4295477	Overturned
278	58	-5058839	4309923	Normal
290	56	-5058839	4309183	Normal
15	84	-5070507	4304103	Normal
55	38	-5068540	4303088	Normal
100	24	-5042435	4302780	Normal
290	40	-5006282	4275971	Normal
285	30	-5004728	4277823	Normal

270	12	-5003901	4279377	Normal
270	12	-5000420	4281284	Normal
280	50	-5023917	4280733	Normal
280	30	-5022759	4283313	Normal
265	20	-5021304	4284967	Normal
280	25	-5020378	4286720	Normal
95	60	-5015053	4290258	Normal
240	35	-4986561	4299929	Normal
275	40	-4983451	4301490	Normal
270	32	-4953188	4289308	Normal
280	34	-4965825	4289162	Normal
275	37	-4949805	4291651	Normal
280	55	-4954884	4290829	Normal
270	22	-4957282	4291131	Normal
260	60	-4950720	4295223	Normal
70	65	-4962107	4293085	Normal
60	45	-4961811	4295070	Normal
70	85	-4947968	4297737	Normal
275	60	-4952730	4298965	Normal
270	39	-4958043	4299346	Normal
270	10	-4955249	4302076	Normal
270	69	-4966150	4284082	Normal
270	54	-4963852	4287638	Normal
310	33	-5068797	4306758	Normal
310	80	-5064173	4314694	Normal
310	37	-5069413	4320796	Normal
310	44	-5054718	4314211	Normal
310	21	-5083083	4291851	Normal
130	20	-5084601	4290815	Normal
130	80	-5085843	4289849	Normal
310	25	-5081426	4293438	Normal

Datum: WGS 1984
Projection: Albers Equal Area Conic

7.2. Data and Methods

7.2.1. *Geologic Maps*

The geologic relationships of the Dang Valley area were investigated using multiple geologic maps of the Dang Valley area which include: the Geologic Map of Nepal (scale: 1:1,000,000) was initially used and provided geologic data where detailed studies were not available; the Geologic Map of Western Central Nepal (Tater et al., 1983) provides more detailed contacts and dip data from the western portion of the study area.

A study completed by Mugnier et al. (1999) provided additional dip data and locations of major faults over the entire study area. The map shows Lower, Middle and Upper Siwalik lithological boundaries. A detailed geologic map by Regumi et al. (2011) is used to the south and west of the Dang Valley. This map provided detailed lithological contacts using the more detailed stratigraphy developed by Dhital et al. (1995). The map also identified the locations of faults and overturned beds based on the detailed stratigraphy. Multiple faults identified by Mugnier et al. (1999) are not observed on this map.

A map of the Surai Khola area is completed by Nakayama and Ulak (1999) using the detailed lithology from Dhital et al. (1995). Faults are identified but hanging wall and footwalls are not marked and no strike and dip data are provided.

These maps were integrated into ArcGIS to create one basemap combining all the contacts, faults, and strike and dip data. When a discrepancy between the map data was identified the more detailed geologic map is favored. For example, the geologic map of the central section (Regumi et al., 2011) was favored over the regional geologic map

(Mugnier et al., 1999). Regumi et al. (1999) observed overturned bedding which led to a different interpretation of fault orientations than Mugnier et al. (1999).

7.2.2. *Kinematic Modeling - Assumptions and Uncertainty*

In order to construct kinematic models and cross sections based on large scale structures without detailed timing information, the following assumptions and uncertainties are applied to this research:

1. The kinematic models and cross sections represent schematics of the structures formed using the fault bend fold model and the fault propagation model and, therefore, does not account for small scale fold and faults that have been observed in the study area (Regumi et al., 2011).
2. Shortening is assumed to occur only in the orientation of the cross sections. Any out of plane motion or ductile deformation is not accounted for in this research.
3. Rates of erosion and variations in stratigraphic thickness of synorogenic deposits were not incorporated into the models. One thickness measurement is used for each cross section based on stratigraphic measurements in that area.
4. There is evidence in the field of multiple detachment levels within Ls (Mugnier et al, 1999; Regumi et al., 2011). This is ignored in the models because details of this data were not provided and at the scale of the structures modeled. The depth to detachment difference in Ls would not have affected the final geometries of the models produced.

5. Field work was not conducted in this study. All data used came from published geologic maps and published research. The quality of the interpretation is only as accurate as the data provided on the geologic maps and the accuracy of georeferencing in ArcGIS 10. Strike and dip data provided may represent small scale features such as local folding and faulting and may not be representative of the regional geologic trends and structures.

8. REFERENCES

Auden, J. B., 1935. Traverses in the Himalaya. Rec. Geol. Surv. India 69, 123-167.

Avouac, J. P., 2003. Mountain building, erosion and the seismic cycle in the Nepal Himalaya. Adv. Geophys. 46, 1–80.

Bilham, R., Larson, K., Freymueller, J., and members, P. I., 1997. GPS measurements of present-day convergence across the Nepal Himalaya. Nature 386, 61–64.

Calassou, S., Larroque, C., Malavieille, J., 1993. Transfer zones of deformation in thrust wedges: an experimental study. Tectonophysics 221, 325-344.

Chen, W.P. and Yang, Z., 2004. Earthquakes beneath the Himalayas and Tibet: Evidence for strong lithospheric mantle. Science 304:5679, 1949-1952.

Corvinus, G., 1988. The Mio-Plio-Pleistocene litho- and biostratigraphy of the Surai Khola Siwaliks in West Nepal: first results. C.R. Acad. Sci. Paris 306, 1471-1477.

Crampton S, L., and Allen, P. A., 1995. Recognition of flexural forebulge unconformities in the geologic record. AAPG Bull., 79, 1495-1514.

Currie, B. S., 1997. Sequence stratigraphy of nonmarine Jurassic-Cretaceous rocks, central Cordilleran foreland-basin system. Geol. Soc. Am. Bull., 109, 1206-1222.

Dahlen, F.A., 1990. Critical taper model of fold-and-thrust belts and accretionary wedges. Annu. Rev. Earth Planet. Sci 18, 55-99.

Davis, D., Suppe, J., and Dahlen, F.A., 1983. Mechanics of fold-and-thrust belts and accretionary wedges. Journal of Geophysical Research 88, 1153-1172.

DeCelles, P. G. and Giles, K. A., 1996. Foreland basin systems. Basin Research 8, 105–123.

DeCelles, P. G., G. Gehrels, J. Quade, and T. Ojha, 1998a. Eocene-early Miocene foreland basin development and the history of Himalayan thrusting, western and central Nepal. Tectonics 17, 741–765

DeCelles, P.G., Gehrels, G.E., Quade, J., Ojha, T.P., Kapp, P.A., and Upreti, B.N., 1998b. Neogene foreland basin deposits, erosional unroofing, and the kinematic history of the Himalayan fold-thrust belt, western Nepal. Geological Society of America Bulletin 110, 2-21.

Delcaillau, B., Herail, G., Mascle, G., 1987. Evolution geÂomorphos-tructurale de fronts de chevauchements actifs: le cas des chevau- chements intra-Siwalik du NeÂpal central. Zeitschrift fuÈ r Geomorphologie Neue Forschung 31, 339-360.

Dhital, M.R., Gajural, A. P., Pathak, D., Paudel, L. P. and Kizaki, K., 1995. Geology and structure of the Siwaliks and Lesser Himlaya in the Surai Khola-Bardanda area, Mid-Western Nepal. Bull. Dept. Geology, Tribhuvan Univ. 4, 1-70.

Gautam, P. and Appel, E., 1994. Magnetic polarity stratigraphy of Siwalik Group sediments of the Tinau Khola Section in West Central Nepal, revisited. Geophys. Jour. Int. 117, 223 -234.

Harrison, T.M., Copeland, P.,Hall, S.A.,Quade, J., Burner,S.,Ojha,T.P.,and Kidd,W.S. F., 1993. Isotopic preservation of Himalayan/Tibetian uplift, denudation, and climatic histories in the two molasses deposits. Jour. Geol. 101, 157-175.

Hodges, K. V., Hurtado, J. M., and Whipple, K. X., 2001. Southward extrusion of Tibetan crust and its effect on Himalayan tectonics. Tectonics 20, 799-809.

Horton, B. K., and P. G. DeCelles, 1997. The modern foreland basin system adjacent to the Central Andes. Geology 25, 895-898.

Jouanne, F., Mugnier, J. L., Gamond, J. F., Fort, P. L., Pandey, M. R., Bollinger, L., Flouzat, M. and Avouac, J. P., 2004. Current shortening across the Himalayas of Nepal. Geophysical Journal International 157, 1–14.

Larson, K.P., Godin, L., Davis, W.J., and Davis, D.W., 2010. Out-of-sequence deformation and expansion of the Himalayan orogenic wedge: insight from the Changgo culmination, south central Tibet. Tectonics 29, TC4013.

Lave´, J., and Avouac, J.-P., 2000. Active folding of fluvial terraces across the Siwaliks Hills, Himalayas of central Nepal. J. Geophys. Res 105, 5735–5770.

Liu, G., and Einsele G., 1994. Sedimentary history of the Tethyan basin in the Tibetan Himalayas. Geol. Rundsch. 83, 32–61.

MapPoint Nepal, 2004. Geologic Map of Nepal, scale 1:1,000,000, 1 sheet

Mugnier, J.L., Leturmy, P., Mascle, G., Huyghe, P., Chalaron, E., Vidal, G., Husson, L., Delcaillau, B., 1999. The Siwaliks of Western Nepal: I. geometry and kinematics. Journal of Asian Earth Sciences 17 (5-6), 629-642.

Nakayama, K., Prakash, U.D., 1999. Evolution of fluvial style in the Siwalik Group in the foothills of the Nepal Himalaya. Sedimentary Geology 105, 205-224.

Pandey, M.R., Tanduker, R.P., Avouac, J.P., Vergne, J., and Heritier, Th., 1999. Seismotectonics of the Nepal Himalaya from a local seismic network. Journal of Asian Earth Sciences 17, 703-712.

Powell, C. McA., and P. J. Conaghan, 1973. Plate tectonics and the Himalayas. Earth Planet. Sci. Lett., 20, 1- 12.

Regumi, D.A., Dhital, R.M, Gadtaula, R., Tamraker, K.N., Yoshida, K., 2011. Lithostratigraphy and structures of the Siwaliks rocks in the southern part of Dang

and its surrounding area, Southwestern Nepal. Journal of the Faculty of Science Shinshu University 43: 1-42.

Robinson, D.M., 2008. Forward modeling the kinematic sequence of central Himalayan thrust belt, western Nepal. Geosphere 4, 785-801.

Robinson, D.M., DeCelles, P.G., Patchett, P.J., and Garzione, C.N., 2001. The kinematic history of the Nepalese Himalaya interpreted from Nd isotopes. Earth and Planetary Science Letters 192, 507–521.

Robinson, D.M., DeCelles, P.G., and Copeland, P., 2006. Tectonic evolution of the Himalayan thrust belt in western Nepal: Implications for channel flow models. Geological Society of America Bulletin, 118, 865–885.

Styron R.H., Taylor M.H., Murphy, M.A., 2011. Oblique convergence, arc-parallel extension, and the role of strike-slip faulting in the High Himalaya. Geosphere 7(2), 582-596.

Tater, J.M., Shrestha, S.B., Shrestha, J.N., 1983. Geologic Map of Western Central Nepal. Department of Mines and Geology, scale 1:250,000, 1 sheet.

Tandon, S.K., 1990. The Himalayan foreland: focus on Siwalik basin, in: Tandon, S.K., Pant, C.S., Casshyap, S.M. (Eds.), Sedimentary basins of India: tectonic context. Gyanodaya Prakashan Print, Nainital, pp. 171-201.

Turcotte, D. L., and G. Schubert, 1982. Geodynamics: Applications of Continuum Physics to Geological Problems, 450 pp., John Wiley, New York.

Upreti, B.N., 1999. An overview of the stratigraphy and tectonics of the Nepal Himalaya. Journal of Asian Earth Science 17, 577–606.

West, R. M. and Munthe, J., 1981. Cenozoic vertebrate paleontology and stratigraphy of Nepal. Himalayan Geology 11, 18-27.

Wobus, C.W., Hodges, K.V., Whipple, K.X., 2003. Has focused denudation sustained active thrusting at the Himalayan topographic front? Geology 31, 861– 864.

Wobus, C., Heimsath, A., Whipple, K., Hodges, K., 2005. Active out-of-sequence thrust faulting in the central Nepalese Himalaya. Nature 434, 1008–1011.